

ARTICLES

Scale Dependence of Lithological Control on Topography: Bedrock Channel Geometry and Catchment Morphometry in Western Scotland

John D. Jansen, Alexandru T. Codilean,¹ Paul Bishop, and Trevor B. Hoey

*Department of Geographical and Earth Sciences, University of Glasgow, Glasgow G12 8QQ, United Kingdom
(e-mail: john.jansen@ges.gla.ac.uk)*

ABSTRACT

We propose that a scale-dependent topographic signature of erodibility arises due to fluvial and glacial erosion acting on different parts of the landscape at different times. For 14 catchments in western Scotland, we define three levels of substrate erodibility in order of decreasing resistance: quartzite rocks, nonquartzite rocks, and zones of fault-related fracture. Then, using digital topographic and planimetric data coupled with field measurements, we identify regression-based scaling relationships between substrate erodibility and morphometric parameters at two spatial scales. Catchment-scale morphometry shows a weak to variable relationship with substrate metrics overall. Erodeability can be inferred from catchment steepness indices (i.e., channel steepness index and relief ratio), but the existence of multiple exceptions could confound a more general application of this approach. Nonetheless, major valley troughs trace fault zones and nonquartzite rocks, leaving much of the higher and steeper ground formed in quartzite. At the reach scale, bedrock channel slope is far more sensitive to substrate erodibility than is channel width. Quartzite outcrops steepen bedrock channels by a factor of 1.5–6.0, and in terms of unit stream power, channels increase their erosional capacity by a factor of 2.7–3.5. Yet only 4%–13% of this increase is due to channel narrowing. Based on a large data set of bedrock channel width ($n = 5825$) from four rivers, we find that width scales with drainage area (in m^2) as $W = 0.01A^{0.28}$. Our results are consistent with the view that width-area scaling is similar in all single-thread rivers subject to transport-limited conditions but that for increasingly sediment supply-limited settings, erosional thresholds at the channel boundary are the key determinants of bedrock channel width.

Introduction

Much of geomorphology is focused on quantifying the forces involved with shaping topography, especially those associated with erosion by water and ice. Less attention is directed at understanding and quantifying the resistance to these forces due to the lithological structure and materials of the Earth's crust (Selby 1980; Moglen and Bras 1995; Molnar et al. 2007). Yet the role of differential resistance to erosion is recognized in the earliest qualitative explanations of landscape evolution (e.g., Gilbert 1877; Davis 1899). Hack's (1960, 1975) dynamic equilibrium model, which refines Gilbert's earlier ideas, argues that hillslope angle is a function of the relative erodibility of the substrate, and that

“every slope and every channel is adjusted to every other” (Hack 1960, p. 80). The Hack model links steeper hillslopes and higher topographic relief with low erodibility, a prediction supported by numerical simulations and empirical data that show hillslope height and topographic relief are a non-linear function of rock mass strength (Selby 1980; Schmidt and Montgomery 1995; Korup 2008). In steep terrain, valley floors set the lower boundary to which hillslopes adjust, so any discussion of substrate controls on hillslope morphology pertains equally to bedrock river profiles (Whipple and Tucker 1999).

A further aspect linking the early landscape evolution models is that they are formulated on the persistently long-lived topography of ancient orogenic belts. The longevity of non- or postorogenic mountain belts is variously attributed to the iso-

Manuscript received August 18, 2009; accepted January 6, 2010.

¹ Present address: GFZ German Research Centre for Geosciences, Telegrafenberg, 14473 Potsdam, Germany.

static response of deep crustal roots (Stephenson 1984), postorogenic uplift (Pazzaglia and Gardiner 1994) including flexural isostasy (Summerfield 1991), and the varying rates of surface processes across the landscape (Crickmay 1975; Twidale 1976, 1991; Baldwin et al. 2003). A characteristic feature of old mountain belts is their high rock mass strength, particularly where deeply exhumed Precambrian crystalline and metamorphosed quartzites are exposed at the surface (Summerfield 1991; Clayton and Shamoon 1998). Notwithstanding the numerous regional studies linking topography to structure, the implications of lithological controls for non- or postorogenic landscapes, generally, are yet to be fully explored.

The influence of substrate erodibility on landscape morphology is emphasized by Molnar et al. (2007) who argue that rock fracture during deformation is the fundamental tectonic control on landscape evolution because the resultant decrease in rock mass strength predisposes valleys and hillslopes to rapid erosion. The argument applies both to rocks actively deforming today and to rocks deformed during orogenies long ago. This being so, an understanding of how substrate erodibility influences landscape evolution is a central question in geomorphology pertinent to all tectonic settings. Here, in the context of postorogenic western Scotland, we examine the topographic signature of substrate erodibility at spatial scales ranging from whole-of-catchment to bedrock channel reach slope and width.

Substrate Erodibility Effects and Scale Dependence. Quantifying the relationship between substrate erodibility and topography is not straightforward because resistance is nonuniform across the landscape, and the main erosional agents—rivers, debris flows, landslides, and glaciers—operate at different spatial and temporal scales. For example, on the bed of a steep river or glacier, intergranular strength controls abrasion rates (length scale $<10^{-3}$ m; Hallet 1981; Sklar and Dietrich 2001), joint-spacing controls quarrying (10^{-2} to 10^0 m; Wohl and Ikeda 1998; Whipple et al. 2000), and the internal friction of hillslopes—a function of fracture spacing due to joints or bedding planes (10^1 to 10^6 m)—controls shallow bedrock landsliding (Selby 1993). The latter is thought ultimately to determine the height of kilometer-scale bedrock hillslopes (Schmidt and Montgomery 1995). However, neither the mechanics nor the scale dependence of any of these erosional processes is understood in detail. Scale-related issues pose difficulties for parameterizing erodibility in numerical simulations of landscape evolution and partly explain the

tendency to assume “uniform erodibility,” a simplification that may be ignoring a critical aspect of the controls on topography in most, if not all, landscapes (Stock and Montgomery 1999; Molnar et al. 2007). Understanding the spatial scales over which substrate erodibility influences landscapes is crucial for linking reach-scale process-form associations to catchment-scale morphology in quantitative landscape evolution models (Dietrich et al. 2003).

The majority of studies on the relationship between substrate erodibility and topography are concerned with what controls steepness and therefore how substrate affects relief development. Yet more than a century of research has produced little consensus on this point. In principle, lithological control of topography will be clearest where rock is widely exposed (i.e., where it is weathering/detachment limited) relative to areas mantled with sediment (i.e., transport limited). Rock exposure on slopes or in channels is dependent on the rate of sediment removal (q_c) exceeding the rate of sediment production or supply (q_s), which are together a function of soil production, rock mass strength, rock uplift rate, river discharge/debris flow/landslide magnitude-frequency attributes, and inherited factors linked to Quaternary climate change. Consider that each of these variables involves several interacting factors and it becomes apparent why, with differing expressions of the ratio q_s/q_c , most landscapes comprise a mosaic of forms reflecting variable degrees of lithological control. Moreover, if the rock mass strength pertinent to hillslope internal friction is distinct from that which controls erosion thresholds on a river bed, it follows that the topographic effects of a particular lithology will differ depending on whether it crops out on a hillslope or in a river channel. To explore this point a little further, we briefly review how the effects of substrate erodibility differ for hillslopes and river channels.

Sediment-mantled hillslopes erode via diffusion-like processes, such as creep and slope wash (Fernandes and Dietrich 1997), but steepening brings rock rapidly to the surface. The development of rock strength equilibrium hillslopes at relatively low rates of rock uplift (>0.2 mm/yr) means that hillslope inclination in steep mountain belts is widely insensitive to uplift and is largely a function of landslide frequency (Burbank et al. 1996; Montgomery and Brandon 2002). Analyzing the distribution of slope angles relative to lithology in New Zealand, Korup (2008) contends that the hillslope inclination threshold for landsliding is set by spatial patterns of erodibility, irrespective of rock up-

lift rate or climate. Support for such broad-scale lithological control on topography comes from a regional-scale analysis of the central European Alps in which Kühni and Pfiffner (2001) find that lithological controls strongly influence relief and key aspects of drainage network; conclusions that reiterate those of numerous studies of the Alps dating back to the 1930s (see references in Kühni and Pfiffner 2001). Furthermore, strong lithological control is not limited to active mountain belts. As shown by Clayton and Shamoon (1998, 1999), differential erodibility governs much of the regional-scale relief structure of the British Isles.

Turning now to rivers, Hack's (1957) work in Virginia and Maryland finds that for a given drainage area, progressively steeper slopes and coarser bed materials occur in streams flowing over limestone, shale, and sandstone, and in nearby Pennsylvania, Brush (1961) finds that stream profiles over shales are more concave than those on comparatively resistant sandstones and limestones. Other examples of lithology influencing channel concavity (and steepness) are documented for streams draining the Santa Ynez Mountains, California (Duvall et al. 2004), and the Oregon coastal mountains (VanLaningham et al. 2006), and Miller (1958) demonstrates an important role for lithology in channel slope and morphology in the Sangre de Cristo Range, New Mexico. On the other hand, Brookfield (1998) argues for absence of lithological control of regional-scale river slopes fringing the Himalayas in favor of discontinuities being the product of differential rock uplift or river capture. Likewise, Chen et al. (2003) finds that lithological control on channel slope is subordinate to tectonic forcing in Taiwan's Western Foothills, though resistant rocks cause local steepening along a small tributary of the Chishue River. In an extensive analysis of river profiles at the eastern edge of the Tibet plateau, Kirby et al. (2003, p. 16) reports that "lithological variations do not appear to account for the systematic regional patterns in channel steepness indices." Yet they draw two striking examples of pronounced steepening along ~20- and ~40-km reaches crossing massive unjointed rocks (Kirby et al. 2003; their fig. 10), and speculate that many other examples exist.

Generalizing so far: first we note that the influence of substrate erodibility applies irrespective of any particular tectonic or climatic setting and over a range of spatial scales from the relief structure of mountain belts to the texture of channel sediments. Second, large-scale analyses focusing on hillslopes (or whole-landscape morphometry) tend to emphasize lithological control on topography and relief,

whereas rivers tend to respond more variably to substrate erodibility. Reasons for this difference probably lie with the complex array of variables that determine river profiles (cf. eq. [5] below), and particularly the incidence of detachment-limited versus transport-limited bedrock river incision. Steepland rivers perform the dual function of eroding bedrock while also removing debris supplied from upstream and adjoining slopes. Lithology controls channel slope chiefly by governing thresholds for bedrock detachment but also by influencing the size and therefore mobility of channel alluvium that shields the underlying bedrock from erosion (Hack 1957; Sklar and Dietrich 1998, 2001). Consequently, the state of the channel bed is likely to have a large bearing on how strong-rock outcrops affect channel geometry. The high erosion thresholds that promote steep channels under detachment-limited conditions are suppressed along reaches blanketed with sediment, wherein channel slope becomes a function of sediment flux (Howard 1980). Thresholds of bedrock erosion and sediment entrainment are shown by numerical simulations to be major determinants of bedrock river incision rates (Tucker and Whipple 2002; Snyder et al. 2003b), and allied thresholds probably also govern channel width (Montgomery 2004). The key role of erosional thresholds extends also to landscapes shaped by ice. Although glaciers are less subject to sediment transport capacity limits, compared to rivers, glacial erosion is certainly limited by detachment thresholds for bedrock erosion, as shown by several studies describing lithological control on glacial trough cross sections and long profiles (e.g., Augustinus 1992, 1995).

In this study we investigate how substrate erodibility (i.e., rock-type and fault-related fracture) is expressed in the erosional topography of glaciated, postorogenic western Scotland. Considerations of scale are central to this question because the erosional agents, rivers and glaciers, act on different parts of the landscape at different times. Catchment-scale topography is the product of preglacial times (>2.5 Ma) overprinted by multiple glacial-interglacial stages, whereas the reach scale reflects the fluvially dominated postglacial regime (<10 k.yr.). We employ digital topographic and planimetric data, coupled with field measurements, to identify differences in the strength of lithological controls in 14 catchments at two spatial scales. At the catchment scale we evaluate whether substrate erodibility is the major determinant of landscape morphology (i.e., drainage area, relief, hypsometry, steepness, and concavity); we then focus on the reach-scale bedrock channel geometry, the scale at

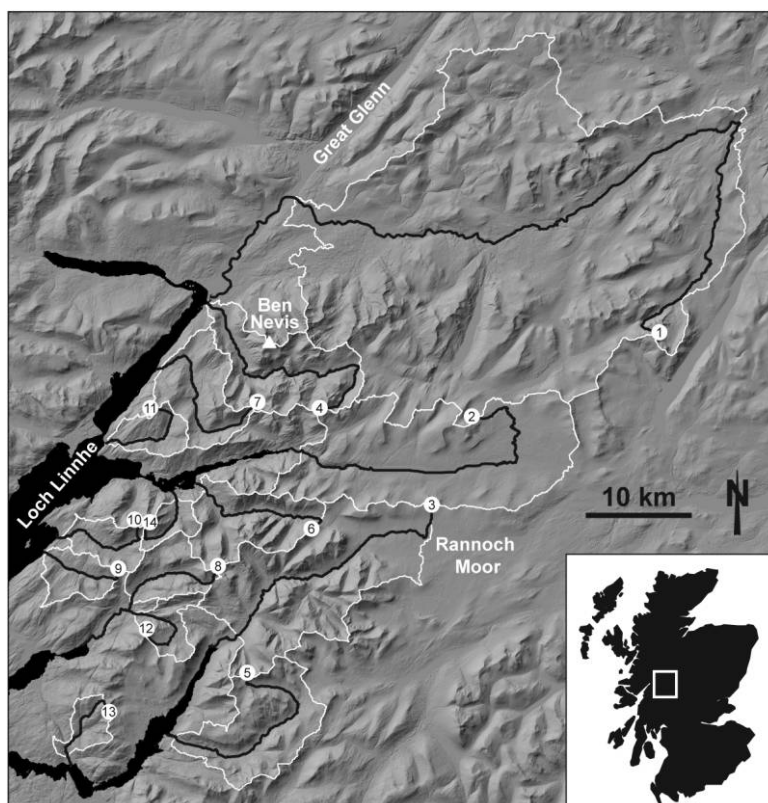


Figure 1. Location of the 14 study catchments (*white outlines*) draining to Loch Linnhe, the largest of Scotland's west coast fjords. The main trunk channels (*black lines*) are numbered and keyed to table 2. Ben Nevis (1343 m) is the highest peak in the British Isles. The background is a shaded relief image derived from a NEXTMap digital elevation model.

which many river incision models are formulated (note we use the abbreviated term “bedrock channel” to mean what is more correctly termed “mixed bedrock-alluvial channel”). Utilizing a simple unit stream power-based model that explicitly incorporates local variations in bedrock channel width, we quantify the relative contribution of channel width and slope to adjustments in erosional capacity where (four) rivers traverse resistant bedrock. We find that unit stream power increases by a factor of 2.7–3.5 at strong rock outcrops mainly via channel steepening rather than channel narrowing. Our bedrock channel-width data support the notion that width-area scaling is similar in all single-thread rivers subject to transport-limited conditions but that for sediment supply-limited settings, erosional thresholds at the channel boundary are the key determinants of bedrock channel width.

Study Area

The study area lies to the west of Loch Linnhe, the largest of the fjords in the western Highlands of

Scotland (fig. 1). We selected the 14 largest river catchments with drainage areas of 10–820 km². From sea level the hills rise abruptly to over 1.3 km at Ben Nevis, inducing orographic precipitation of 2.2–3.2 m yr⁻¹ across some of the wettest and most rugged terrain in the British Isles.

Geology and Morphotectonics. The Scottish Highlands constitute a small remnant of the deeply eroded Caledonian mountain belt, now positioned at Europe's northwest rifted margin. Outlines of relief and drainage follow the ~NE-SW trend in the dominant fold and fault structures (Harris 1991). The Great Glen Fault, the major structural feature crossing the study area, divides the Moinian rocks to the northwest from the Dalradian rocks of the study area (fig. 2). The Dalradian (700–450 Ma) is a varied group of rocks folded into a series of nappes, which in the study area comprise mainly schists and metaquartzites (the Appin, Argyll, and Grampian groups; see table 1) intruded by Silurian-Devonian igneous complexes and overlain by Devonian lavas (Harris et al. 1994).

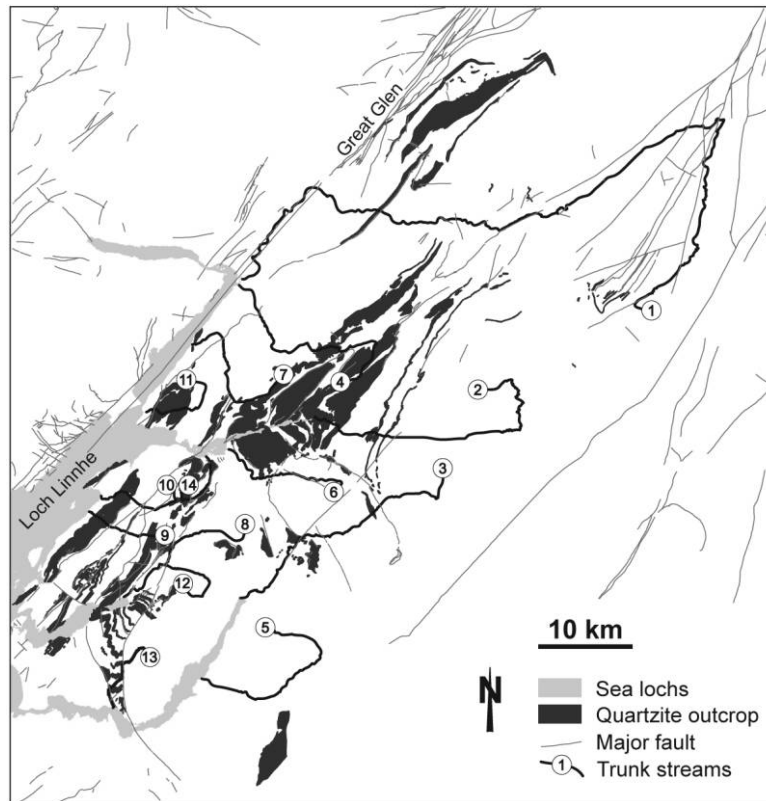


Figure 2. Schematic geology map based on 1 : 50,000 British Geological Survey sheets and showing major faults and quartzites generalized from the 31 lithologies listed in table 1.

Scotland is largely tectonically quiescent, consistent with its position at a passive continental margin. The last phase of major tectonism occurred with the passage of the ancestral Iceland mantle plume during the early Palaeogene, when large-scale volcanism and mantle underplating is thought to have caused >350 m of surface uplift (Stuart et al. 2000; Persano et al. 2007). Consequently, a pulse of rapid denudation between 61 and 50 Ma is reported from apatite (U-Th)/He and fission track analyses; however, with maximum post-Mesozoic denudation of just 1330 ± 230 m, the Cenozoic is characterized by slow denudation overall (Persano et al. 2007). Glacio-isostatic rebound has driven brief intervals of rock uplift rates up to 9 m/k.yr. during the Late Devensian deglaciation (~13 k.yr.) declining to 2–1 m/k.yr. in the study area today (Shennan et al. 2000; Firth and Stewart 2000). Although rapid, this uplift pulse is too brief to affect large-scale topographic relief, so we consider rock uplift in this landscape to be essentially spatially invariant since the early Paleogene. The fluvial incisional response associated with glacio-isostatic rebound is restricted to areas

close to base level; such areas are excluded from this study, and we report on this topic elsewhere.

Glacial Erosion. More significant for topography are the effects of glacial erosion since the advent of midlatitude ice sheet glaciation at ~2.4 Ma (Shackleton et al. 1984), with the most recent ice-sheet decay in the Scottish Highlands at the close of the Younger Dryas stadial (Golledge et al. 2007). The Loch Linnhe study area is within the most heavily glaciated part of the British Isles (Clayton 1974). The regional distribution of glacial erosion is interpreted to reflect the dynamics and basal thermal regimes of successive ice sheets (Sugden and John 1976). Selective linear erosion by ice over recurrent glaciations exploited the NE-SW lines of weakness in the basement rocks, widening and deepening preexisting fluvial valleys (Thomas et al. 2004) and yielding deep glacial troughs and rock basins now flooded by the sea and a western coastline indented with fjords (Gregory 1927). Several valleys exceed a 1-km depth, but how much of this is solely attributable to glaciers is unknown (Boulton et al. 2002).

Erosional Resistance and Topography in Western

Table 1. Thirty-One “Quartzite” Lithologies from the Dalradian Supergroup Generalized into a Single Erosion-Resistant Class of Outcrops

| Group | Lithology |
|-------------------------------------|----------------------------------------------------------------------------------------------|
| Appin: | |
| Appin Quartzite Mm | Quartzite ^a |
| Binnein Quartzite Mm | Metaquartzite ^a |
| Eilde Quartzite Mm | Metaquartzite; ^a feldspathic quartzite ^a |
| Glencoe Quartzite Mm | Metaquartzite ^a |
| Innse Quartzite Mm | Metaquartzite |
| Leven Schist Fm | Quartzite |
| Reservoir Quartzite Mm | Metaquartzite ^a |
| Spean Viaduct Quartzite Fm | Quartzite |
| Stob Quartzite Mm | Metaquartzite ^a |
| Argyll: | |
| Beinn Churlain Quartzite | Quartzite ^a |
| Beinn Donn Quartzite Fm | Quartzite; ^a semipelite; ^a quartzite |
| Creagan Fm | Metasandstone; ^a metasandstone ^a , metamudstone; semipelite, quartzite |
| Creran Bridge Quartzite Fm | Quartzite, ^a pelite |
| Creran Flags Fm | Quartzite, metasandstone, metamudstone; semipelite, ^a quartzite, pelite |
| Grampian: | |
| Beinn Iaruinn Quartzite Fm | Feldspathic quartzite, semipelite |
| Clachaig Semipelite and Psammite Fm | Quartzite ^a |
| Glen Fintaig Semipelite Fm | Feldspathic quartzite |
| Glen Gloy Quartzite Fm | Feldspathic quartzite |
| Inverlair Psammite Fm | Quartzite; mylonitic quartzite; psammite, quartzite, semipelite |
| Linnhe Quartzite Mm | Metaquartzite, semipelite |
| March Burn Quartzite Fm | Feldspathic quartzite |
| Undifferentiated Grampian Gp | Quartzite |

Note. Mm = member, Fm = formation, Gp = group.

^a Outcrops in trunk channel.

Scotland. Early workers (e.g., Geikie 1901; Bailey and Maufe 1916; Gregory 1927) recognized differential erosion along fault zone “shatter belts” in western Scotland, particularly in Loch/Glen Etive, Loch Leven, and Loch Linnhe (the flooded section of the Great Glen Fault; fig. 2). The rocks along these fault zones are generally highly fractured. Sissons (1967) highlights the major correspondence between outcrop of strong rocks, steep topography, and high relief in much of Scotland, observing that rivers and glaciers have exploited lithological weaknesses traced by the NE-SW structural grain of the country and that Precambrian quartzites are especially resistant to denudation in the Highlands. In the study area, between Glen Nevis and Glen

Coe (fig. 1, catchments 4 and 6), quartzite crops out over much of the high ground, including the summits Sgùrr à Mhaim (1099 m), Am Bodach (1032 m) and Binnein Mòr (1130 m). Quartzites also comprise the most imposing summits in the nearby central Grampians, the northwest Highlands, and the Hebridean isles of Jura, Knapdale, and Islay (Sissons 1967). Sissons’s observations are supported by the findings of Clayton and Shamoon (1998, 1999), who correlate rock age with inferred erosion resistance, showing that differential erodibility governs much of the regional scale (areas >10⁴ km²) relief structure of Britain. Clayton and Shamoon (1998) attribute to Precambrian quartzites the greatest relative resistance of all 71 rock types in Britain with outcrop >500 km², based on a set of metrics linking proximity to base level with the degree to which each rock type forms high ground.

Methods and Approach

Lithological Controls on Erosional Resistance. The comparatively high rock-mass strength of metamorphic quartzites is widely reported (e.g., Annandale 1995). Laboratory experiments indicate that resistance to fluvial abrasion is proportional to rock tensile strength, with quartzites among the strongest rocks tested (e.g., Sklar and Dietrich 2001). As with previous studies that infer erodibility from rock type (e.g., Lague et al. 2000; Kühni and Pfiffner 2001; Korup 2008), we do not test rock strength directly, but as noted above, Precambrian quartzites are held to be the strongest and therefore most erosion-resistant rocks cropping out in the study area. Conversely, intense rock fracture along fault planes has produced breccias with a fine matrix that is relatively erodible due to its susceptibility to chemical alteration. Based on these arguments we accept a priori the greater erosional resistance of Precambrian quartzites, and we ascribe minimum erosional resistance to fault zones containing fractured and/or more closely jointed rocks irrespective of lithology. Lithological factors are therefore generalized here into two end-member classes representing strong and weak substrates.

Geological Information. Geological data, comprising lithology, regolith, and structure (including faults), are derived from British Geological Survey digital geology maps compiled from the original 1 : 50,000 scale maps. Lithological information is generalized to simplify the hundreds of rock types while maintaining accurate positioning of lithological contacts. Quartzite (and similar rock types metaquartzite and metasandstone) is a principal constituent of 31 of the mapped lithologies

in the study area. These lithologies are grouped into a single "quartzite" for the purposes of our analysis (fig. 2) but are listed according to Dalradian lithostratigraphy in table 1. The areal extent of quartzite outcrop in each catchment is measured with Arc/Info software and calculated as a fraction of total catchment area. The length of quartzite outcrop along trunk channels is calculated as a fraction of total stream length. Likewise, the length of trunk channels proximal to fault zones is calculated as a fraction of total stream length; channels are considered to be "fault-affected" within 200 m of an observed or inferred fault. Quartzite areal fraction, quartzite relief fraction, and fault-affected length fraction are referred to together as the "substrate metrics."

River Discharge and Drainage Area. The study area receives a relatively uniform distribution of annual precipitation. To test the applicability of using drainage area as a proxy for river discharge, flow data are analyzed from nine flow gauges in the western Highlands with close to natural flow regime (i.e., natural to within 10% at or exceeding the 5-percentile flow). We find that both the median annual flood ($Q_{0.5}$) and discharge with 0.10 exceedance probability ($Q_{0.1}$) are a linear function of drainage area (A in km^2), given by

$$Q_{0.5} = 1.627A + 7.191 \quad (R^2 = 0.97) \quad (1)$$

and

$$Q_{0.1} = 0.237A - 0683 \quad (R^2 = 0.99). \quad (2)$$

For bedrock channels, we assume that $Q_{0.5}$ is a reasonable representation of the channel-forming discharge. We use equation (1) for calculating the discharge component of unit stream power and in the analysis of channel-width discharge scaling below.

Long Profile and Morphometric Analyses. Elevation, stream length and drainage area data are calculated from the hydrologically corrected (Jenson and Domingue 1988; Tarboton 1997) NEXTMap digital elevation model (DEM), a 5-m grid-scale map derived from airborne interferometric synthetic aperture radar (vertical accuracy RMSE = 1.0 m). The DEM is resampled to derive elevation data at 1-m vertical intervals for calculating local channel slope (Wobus et al. 2006), and 0.1-unit logarithmic-binning is used to smooth the slope-area data following standard procedures (Snyder et al. 2000). Catchment-scale morphometry is summarized in table 2. Excluded from the analysis are river reaches affected by artificial reservoirs and artifacts of averaging area across tributary junctions.

Channel slope–area analyses are used to derive long profile indices based on the empirical power law relationship between channel slope and drainage area (Flint 1974),

$$S = k_s A^{-\theta}, \quad (3)$$

where S is local channel slope, A is upstream drainage area, k_s is the channel steepness index, and θ is the channel concavity index. Numerous studies infer landscape dynamics from channel slope–area analyses; in particular, the positive correlation between channel steepness index and rock uplift rate allows spatial patterns of tectonics to be investigated across large areas (e.g., Snyder et al. 2000; Kobor and Roering 2004). However, as the steepness index is also strongly influenced by erosion resistance and precipitation patterns, a simplification that excludes lithological variation is commonly adopted for the sake of exploring rock uplift. In principle, this approach may be inverted to focus on bedrock erosion resistance: where rock uplift rate and climate are known to be spatially invariant, spatial differences in steepness index become principally a function of lithological resistance (Lague et al. 2000; Snyder et al. 2000). This is the approach we adopt here. Equation (3) describes the concave-up long profiles that are generally found in nonglaciaded landscapes irrespective of substrate or equilibrium conditions. We apply it to glaciaded western Scotland as a simple descriptor of long profile shape, noting that the irregular morphology of many of the long profiles yields k_s and θ values that are outside normally observed values. In order to compare different long profiles, we derive a normalized form of the channel steepness index, S_r , following Sklar and Dietrich (1998),

$$S_r = k_s (A_r^{-\theta}), \quad (4)$$

where A_r is a representative drainage area at the midpoint of the data set (we use $A_r = 10 \text{ km}^2$). Term S_r is directly analogous to k_s normalized by a reference concavity (Snyder et al. 2000), but S_r is preferable when comparing long profiles across a region with highly variable θ (Wobus et al. 2006).

Figure 3 shows a representative long profile with a strong glacial imprint typical of western Scotland. For the purpose of slope-area analysis the profile is segmented into the headwall zone and valley zone (Brocklehurst and Whipple 2007). The boundary separating these two segments is marked by a change in channel slope analogous to the critical area threshold, A_c , but without the transition from colluvial to fluvial processes that is implied by this

Table 2. Catchment-Scale and Reach-Scale Metrics for the 14 Study Rivers in Western Scotland

| River basins | Drainage area (km ²) | Relief (m) | Valley length (m) | Hypsometric integral | Mean slope angle $\pm 1\sigma^a$ | Normalized channel steepness S_r^b | Total concavity C_r^c | Channel concavity index θ^d | Quartzite areal fraction | Quartzite relief fraction | Fault-affected length fraction |
|--------------|-------------------------------------|---------------|----------------------|-------------------------|----------------------------------------|--------------------------------------------|-------------------------------|------------------------------------------|--------------------------------|---------------------------------|--------------------------------------|
| Spean | 821 | 1044 | 63,484 | .398 | 13.8 \pm 9.4 | .019 | .571 | .398 | .050 | .001 | .766 |
| Leven | 192 | 659 | 26,731 | .423 | 10.1 \pm 8.5 | .009 | 1.083 | .444 | .059 | .212 | 0 |
| Etive | 158 | 437 | 21,184 | .395 | 20.9 \pm 13.0 | .015 | .856 | .177 | .036 | .016 | .367 |
| Nevis | 77.0 | 986 | 22,866 | .383 | 24.3 \pm 11.7 | .029 | .519 | .461 | .214 | .288 | .041 |
| Kinglass | 74.2 | 724 | 18,133 | .388 | 19.0 \pm 10.4 | .028 | .433 | .516 | .005 | 0 | .024 |
| Coe | 55.0 | 345 | 12,272 | .392 | 26.4 \pm 12.7 | .023 | .828 | -.054 | .074 | .026 | .370 |
| Kiachnish | 48.3 | 867 | 14,321 | .343 | 20.7 \pm 10.5 | .023 | .521 | .176 | .063 | .107 | .056 |
| Cretan | 29.1 | 739 | 9245 | .369 | 21.4 \pm 10.8 | .038 | .509 | .351 | .083 | 0 | .168 |
| Salachan | 21.9 | 604 | 7130 | .375 | 16.5 \pm 8.7 | .044 | .730 | .357 | .242 | .318 | 0 |
| Duror | 21.7 | 749 | 8788 | .365 | 19.4 \pm 10.9 | .028 | .537 | -.177 | .215 | .053 | .105 |
| Righ | 19.9 | 554 | 8713 | .462 | 16.6 \pm 8.2 | .005 | .560 | .636 | .391 | .202 | 0 |
| Ure | 18.7 | 685 | 7410 | .435 | 20.8 \pm 12.3 | .052 | .727 | .110 | .036 | 0 | 0 |
| Estragan | 14.9 | 599 | 7022 | .566 | 17.0 \pm 8.3 | .100 | 1.038 | -.135 | .241 | .244 | .342 |
| Laroch | 12.8 | 579 | 5988 | .344 | 22.7 \pm 9.5 | .042 | .722 | .251 | .305 | .549 | .743 |

^a Calculated using a moving window of 3×3 pixels (i.e., 225 m², Horn 1981).

^b Normalized channel steepness derived from equation (4).

^c Total concavity is the area defined by the river long profile and a straight line joining the river outlet and channel head.

^d Channel concavity index derived from equation (3).

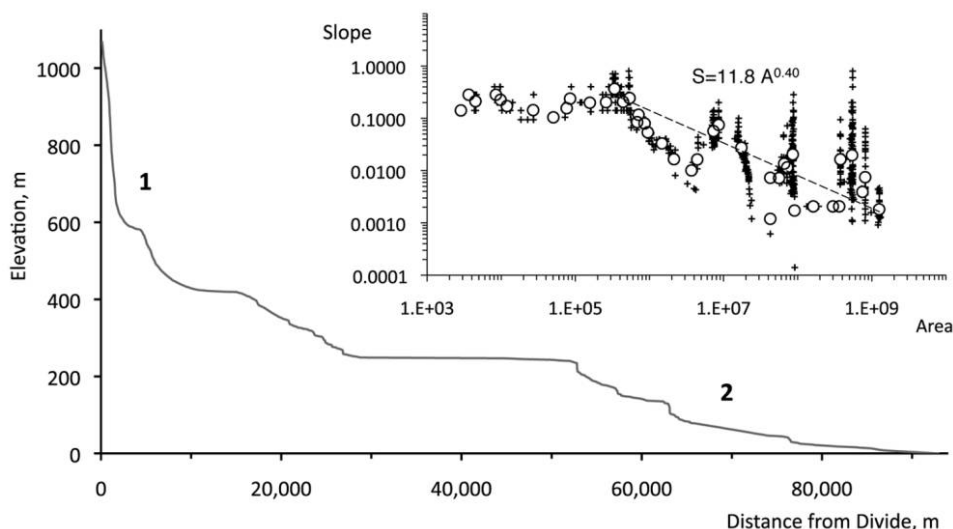


Figure 3. Representative long profile (River Spean), with headwall zone (1) and valley zone (2), indicating a shift from glacially dominated to progressively fluvial downstream. The normalized channel steepness index (S_i) is derived from the slope-area regression combined with equations (3) and (4).

threshold in nonglaciated landscapes. The river profiles in the study area are chiefly glacial in nature, although we speculate that fluvial attributes grow progressively toward the river outlets as a function of the diminishing residence time of valley glaciers downstream and possibly the increasing discharge available to “refluvialize” the landscape.

Modeling Fluvial Erosion. Based on empirical and semitheoretical studies, the factors determining bedrock river incision rate, $\partial z/\partial t$, can be summarized as

$$\frac{\partial z}{\partial t} = f(K_1, q_s, Q, S, W), \quad (5)$$

where K_1 is a substrate erodibility factor, Q is channel-forming discharge, and W is channel width. No river incision model to date successfully incorporates dynamic adjustment of all these variables. Early attempts build on the empirical underpinning of equation (5) to develop a group of “stream power rules” that cast detachment-limited incision rate as a power-law function of bed shear stress or unit stream power (Howard and Kerby 1983; Seidl and Dietrich 1992), with the general form

$$\frac{\partial z}{\partial t} = U - K_2 A^m S^n, \quad (6)$$

where U is rock uplift rate, A is drainage area (a proxy for discharge), m and n are positive exponents

that vary with erosion processes and channel geometry, and K_2 is an erosion efficiency factor that varies over several orders of magnitude and incorporates hydraulic roughness, channel width, catchment runoff attributes, lithological resistance, and sediment load factors (Howard et al. 1994; Stock and Montgomery 1999; Whipple and Tucker 1999). Equation (6) incorporates the downstream variation in channel width into a generic scaling with drainage area via the exponent m . This assumption is valid in relatively uniform lithologies where it has been shown that bedrock channel width increases as a power-law function of discharge in a way similar to the hydraulic geometry relationships for alluvial channels (e.g., Leopold and Maddock 1953). Substituting drainage area for discharge gives

$$W = cA^b \quad (7)$$

where c and b are empirically determined, and several studies report $b \sim 0.3$ – 0.5 (Snyder et al. 2000, 2003a, 2003b; Montgomery and Gran 2001; Tomkin et al. 2003; van der Beek and Bishop 2003).

The inadequacy of equation (6) for fully capturing river behavior is principally due to its lack of accounting for sediment flux and the implicit effect of a fixed K_2 value making channel slope the sole adjustable variable. These are serious flaws because sediment flux is known to be a critical driver of bedrock river incision (Sklar and Dietrich 1998), and field observations in areas of nonuniform rock

strength or tectonic perturbation show that rather than increasing monotonically with drainage area, channel width fluctuates locally in a similar fashion to channel slope (e.g., Harbor 1998; Lavé and Avouac 2001). The second issue can be alleviated by direct measurement of downstream channel-width variation, yielding a unit stream power-based model of detachment-limited bedrock river incision that allows free adjustment of both channel width and slope:

$$\frac{\partial z}{\partial t} = \frac{K_1 Q S}{W}. \quad (8)$$

Rivers are sometimes observed to narrow and/or steepen where they meet resistant bedrock, presumably as a means of increasing boundary shear stress (i.e., erosional capacity) and maintain a constant erosion rate. In order to explore how erosional capacity varies downstream, we calculate unit stream power (ω) with the assumption that erosional capacity is proportional to the downstream growth in discharge along with adjustments in channel width and slope (ignoring momentum losses associated with hydraulic roughness). That is,

$$\omega = \frac{\gamma Q S}{W} \sim \frac{\partial z/\partial t}{K_1}, \quad (9)$$

where γ is the specific weight of water (9807 N/m³) and Q is the channel-forming discharge, as given in equation (1). From downstream variations in ω we then (1) infer substrate forcing of bedrock channel geometry and (2) quantify the relative contribution of channel width and slope to adjustments in erosional capacity at resistant bedrock.

Channel-Width Measurements. Channel-width data derive from British Ordnance Survey Land-Line Plus digital maps, which are available at two scales: 1 : 2500 (x, y relative uncertainty <1.8 m) and 1 : 10,000 (x, y relative uncertainty <4.0 m). Using Arc/Info, a channel centerline parallel to each bank is constructed with nodes at 10-m intervals from the river outlet upstream to a position near the headwaters where channel width falls to <5 m. Channel width is measured at cross sections drawn perpendicular to the banks at each node. River reaches spanning lakes and artificial reservoirs are excluded. This method produces a large number of channel widths along virtually continuous lengths of river channel at 10-m intervals (~5800 channel widths from four rivers are presented here), with the contributing drainage area at each cross section calculated by meshing the DEM with the plani-

metric data. The accuracy of digitally measured channel width is checked with field data (fig. 5).

Lithological and Transient Knickpoints. We adopt the broad definition of a knickpoint as an abrupt change in channel elevation or slope produced by tectonic deformation, base level change, or differential substrate resistance to glacial/fluvial erosion (Howard et al. 1994). It follows that knickpoints divide into two types: transient (disequilibrium) knickpoints that propagate upstream as incisional waves and lithological (static) knickpoints, which do not propagate. This latter type is our focus (fig. 4), though all knickpoints are probably substrate dependent to some degree (Holland and Pickup 1976; Gardner 1983; Wohl et al. 1994; Weissel and Seidl 1997; Bishop et al. 2005; Jansen 2006). All knickpoints involve predominantly detachment-limited bedrock erosion and so are characterized by thin, discontinuous alluvial cover. We visually assessed the extent of alluvial channel cover while walking along the 14 main-stem channels, and we inspected knickpoints for lithological features omitted from the geological maps. Transient knickpoints are caused by spatial or temporal changes in water, ice, or sediment flux at tributary junctions or accelerated relative base level fall (Whipple 2004; Crosby and Whipple 2006). A set of transient fluvial knickpoints close to the study river outlets are the result of base level fall linked to glacio-isostatic rebound, but these are excluded from our analysis.

Results and Analysis

Catchment-Scale Morphometry. Results of the morphometric analyses are summarized in table 2. A selection of the scatterplots (fig. 6) is presented for areal quartzite fraction and fault-affected fraction, for brevity.

Catchment Size and Relief. Drainage area and quartzite areal fraction is inversely scaled (fig. 6a). All large catchments contain <25% quartzite (though some small catchments also contain low quartzite fractions), and fault zones trace the main valley troughs, suggesting that the gross drainage structure is determined by catchment-scale distribution of quartzites and fault-related fracture. Inclusion of the major shatter belts that extend beneath the largest fjords strengthens the scaling between large catchments and fault-affected length (fig. 6b).

Geometry dictates that an increase in maximum catchment relief leads to larger drainage area (fig. 6c), especially where the height of hillslopes is limited by rock mass strength. We find that relief scales

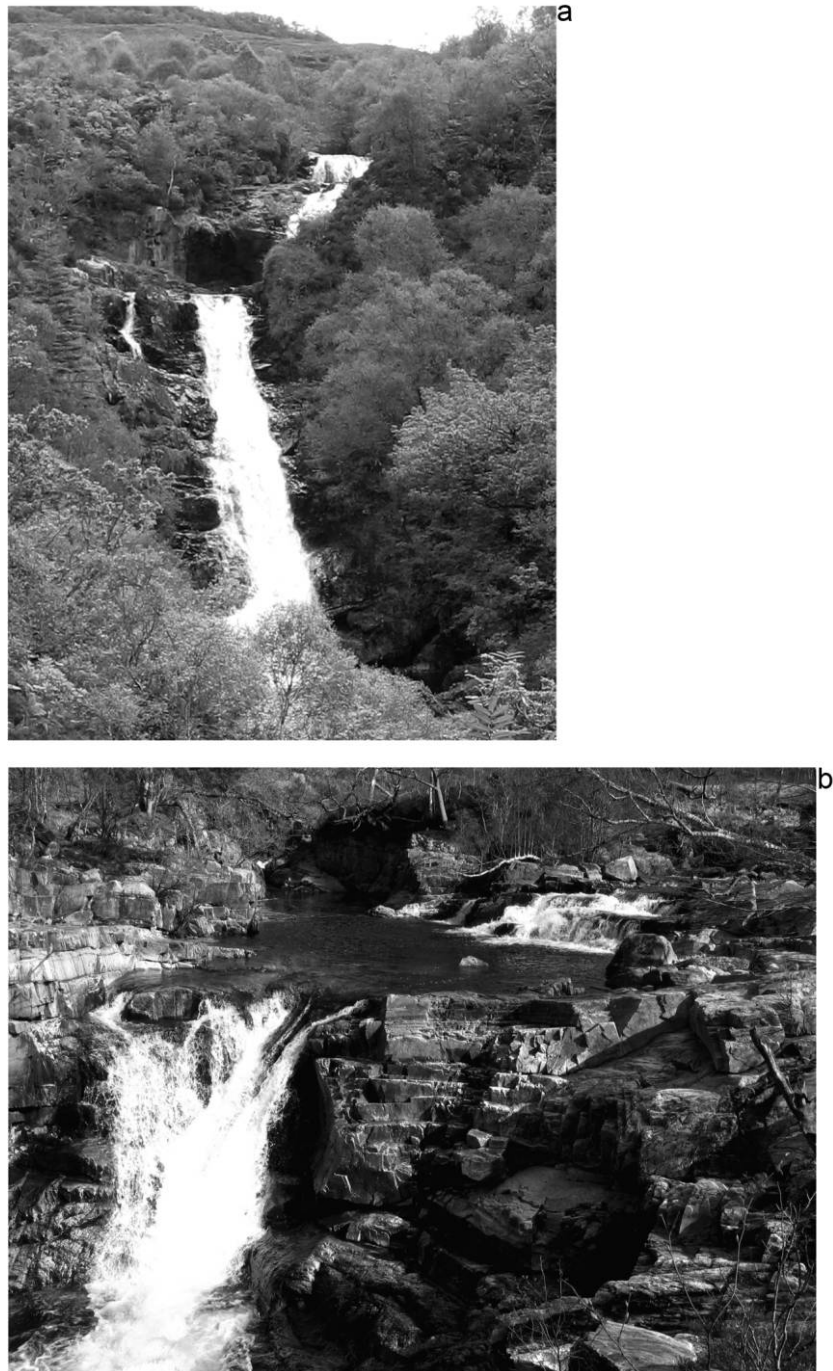


Figure 4. Lithological knickpoints. *a*, Abhainn Rìgh, Glen Rìgh Falls, a 50-m-high waterfall developed on Appin Quartzite; *b*, River Leven at the crest of a 30-m-high waterfall developed on Eilde Quartzite. A color version of this figure is available in the online edition of the *Journal of Geology*.

weakly with substrate metrics, though several outliers occur; in figure 6*c* outliers (2, 3, 6) have their headwaters on the Rannoch pluton, a low-relief granitic basin (fig. 1), and in figure 6*d* the Spean (1) forms a strong outlier.

Mean Slope Angle. Hillslope angle spans 10° – 26° when averaged for each catchment (table 2), a range sufficiently wide to suggest absence of widespread rock strength equilibrium hillslopes. Hillslope inclination is however not independent of

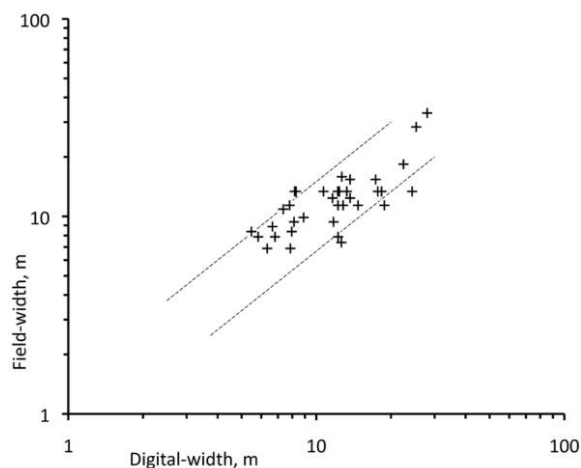


Figure 5. Scatterplot of field-measured channel width versus digitally measured channel width for the rivers Leven, Nevis, and Coe along reaches corresponding to data in figure 8. Field channel width is measured perpendicular to banks using a laser rangefinder or measuring tape. Channel width is defined by the limits of perennial vegetation, indicating the zone of active scour and/or mobile bed material, but more often the channel has two clear bedrock banks. Note that >80% of digitally measured widths fall within 50% of their field-measured values (as indicated by dashes).

substrate erodibility because mean slope angle calculated for quartzite outcrops, 20.0° ($1\sigma = 10.9^\circ$), is steeper than that on nonquartzites, 15.6° ($1\sigma = 10.9^\circ$), though with considerable overlap.

Hypsometry. Catchment hypsometric integrals (H_i) show weak scaling with drainage area (fig. 6e), though three small catchments (11, 12, 13) form outliers, and H_i does not correlate with any substrate metrics (we do not present these plots here). The hypsometric curves themselves are mostly a consistent shape (fig. 6f), suggesting that substrate factors do not control the areal distribution of elevation at catchment scale, aside from the anomalous curves (2, 11, and 13) that correspond to thick quartzite outcrops close to sea level in these catchments. In other words, lithology may strengthen its influence on landscape morphology at the sub-catchment scale ($<10^2$ km²).

Steepness and Concavity Indices. Relief ratio (i.e., maximum relief divided by total stream length) is weakly scaled with quartzite areal fraction (fig. 6g) and largely independent of fault-affected length (fig. 6h). Channel steepness index S_r shows some scaling with quartzite fraction (fig.

6i) but is independent of faults (fig. 6j). The two measures of long profile concavity are both independent of substrate metrics (we do not present these here), and strong linearity is common to many of the long profiles (table 2). Seven of the profiles have C_i (total concavity) values exceeding 0.7 ($C_i = 1$ for a rectilinear profile) and three are convex overall (i.e., negative θ).

Reach-Scale Channel Geometry. Sparse channel sediment storage is characteristic of all 14 rivers. Mixed bedrock-alluvial channels prevail, with alluvial cover thinning or disappearing altogether at knickpoints formed in resistant bedrock. Our observations imply that these rivers are subject to predominantly detachment-limited bedrock erosion and that channel geometry is a function of erosional not depositional processes. To aid comparison between rivers we employ a reference drainage area of 40 km² (close to the median drainage area for the channel-width data set) to calculate 95% confidence intervals for the regression analyses of channel width (W_r), slope (G_r), and unit stream power (ω_r).

Channel Slope. Reach-scale channel slope is measured for the 14 rivers at fixed 1-m vertical intervals downstream, and plotted as average (geometric mean) channel slope per drainage area log-bin (table 3; fig. 7). In figure 7a, 7b, channel slopes across 199 nonquartzite reaches are compared with slopes at 31 major quartzite outcrops as a function of drainage area. The regression analyses, which used

$$S = tA^z, \quad (10)$$

revealed that channel reaches over quartzite are between 1.5 and 6.0 times steeper relative to those over nonquartzite (at $A = 40$ km²), with ranges defined by 95% confidence bands being significantly different, at least for larger streams. The 95% confidence bands merge for drainage areas $<\sim 2.5$ km² and channel slopes steeper than ~ 0.05 , suggesting that erodibility no longer has bearing on channel slope. As with measures of catchment-scale steepness, close proximity to faults appears to have no effect on reach-scale channel slope, with 95% confidence bands defining very similar ranges (fig. 7c; table 3).

Channel Width. Bedrock channel-width data ($n = 5825$) are available for four of the 14 study rivers (table 4). A frequency histogram of reach-scale bedrock channel width yields a gamma-type distribution (fig. 8a), with 75% of bedrock channels

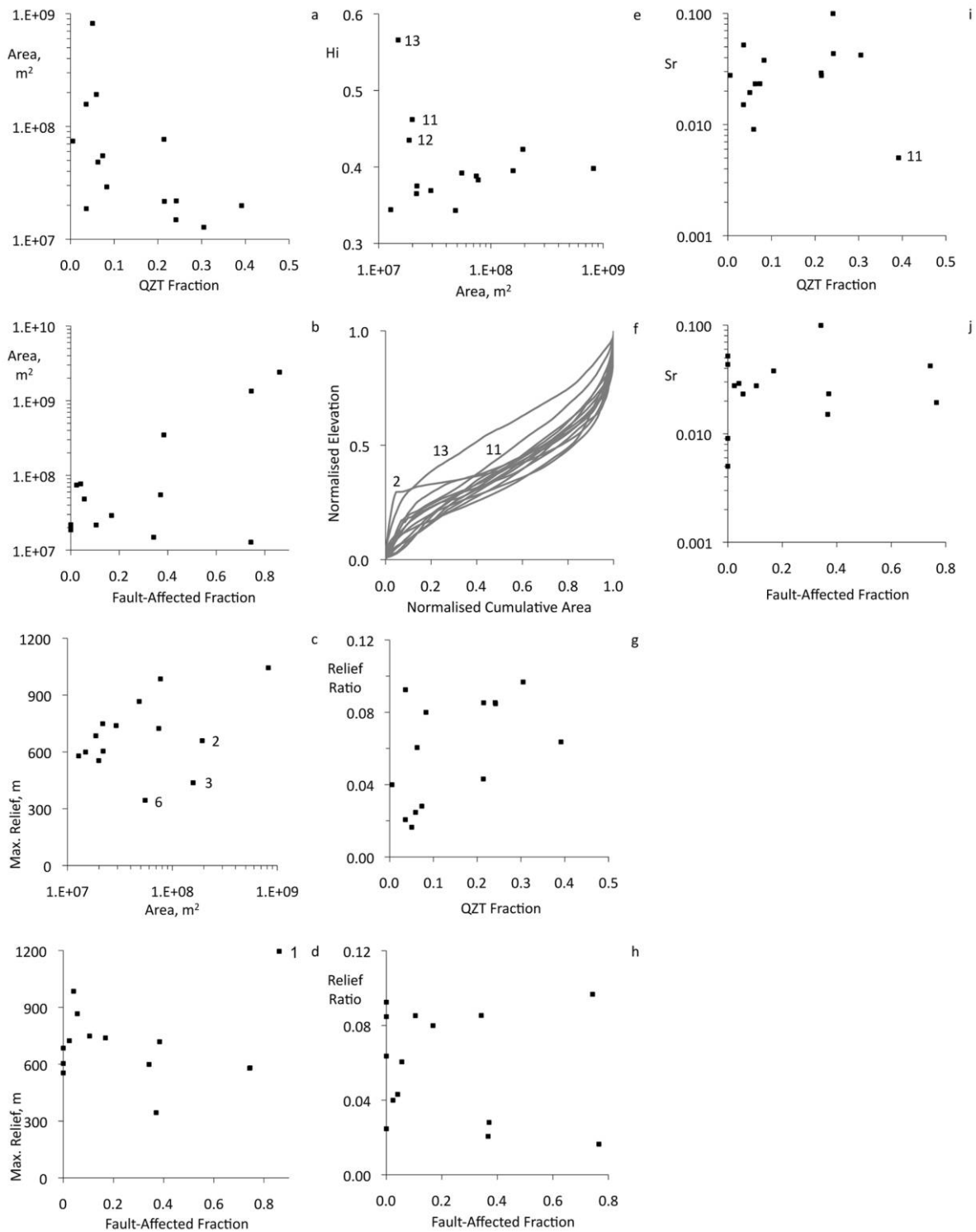


Figure 6. Catchment-scale scatterplots (numbered points are keyed to table 2). *a*, Drainage area versus areal fraction of catchmentwide quartzite; *b*, drainage area versus areal fraction of fault-affected stream length (including fjords); *c*, maximum relief versus drainage area; *d*, maximum relief versus fraction of fault-affected stream length (including fjords); *e*, hypsometric integral (H_i) versus drainage area; *f*, hypsometric curves for each catchment; *g*, relief ratio versus areal fraction of catchmentwide quartzite; *h*, relief ratio versus fraction of fault-affected stream length; *i*, channel steepness index (S_r) versus areal fraction of catchmentwide quartzite; *j*, channel steepness index versus fraction of fault-affected stream length.

Table 3. Regression Analyses of Bedrock Channel Slope S (log-binned) versus Drainage Area A (m^2 , log-binned)

| Substrate | t | z | R^2 | n | Area range (km^2) | $G_r \pm 95\%$ ^a (m) |
|-----------------------------|-------|-------|-------|-----|---------------------------------|------------------------------------|
| Quartzite ^b | 1.14 | -.194 | .17 | 31 | .1–170 | .038 \pm .016 |
| Nonquartzite ^c | 23.9 | -.436 | .43 | 199 | .1–850 | .012 \pm .003 |
| Fault-affected ^d | 331.7 | -.580 | .51 | 36 | 1.7–50.7 | .013 \pm .004 |

Note. The regression analyses are for channel reaches in 14 rivers crossing quartzite and nonquartzite substrates, where $S = tA^z$ (eq. [10]) and $A > 0.1 \text{ km}^2$.

^a G_r is channel slope calculated from regression with 95% confidence interval at a reference drainage area, $A = 40 \text{ km}^2$.

^b River reaches crossing major quartzite outcrops.

^c River reaches crossing nonquartzite rocks.

^d River reaches <200 m from observed or inferred faults, irrespective of lithology.

measuring between 5 and 20 m and just 1.3% exceeding 50 m in width. The power-law scaling between channel width and drainage area indicates that bedrock channel width scales with drainage area, just as in transport-limited channels, though for the rivers analyzed here the value of the exponent lies outside the usually observed $b = 0.3$ – 0.5 (see table 4). Regression of the entire channel width data set yields an exponent value ($b = 0.278$) closer to widely quoted values, and the internal consistency of the results is indicated by a narrow range of W_r (13.2–14.7 m), across all four rivers (table 4). Channels crossing quartzites are between 4% and 13% narrower than those crossing nonquartzites (at $A = 40 \text{ km}^2$), with 95% confidence bands that do not overlap (fig. 8b; table 4). To test for variability in channel-width response to the four different “quartzite” lithologies (table 1), we plot mean channel width versus log-binned drainage area (fig. 8c). The orderly power function shown in figure 8c suggests that the four quartzite lithologies do not differ in their effect on width-area scaling and so justifies grouping them into a single lithology.

Unit Stream Power ω . Results above suggest that substrate is a major determinant of bedrock channel geometry and will be reflected in ω (eq. [9]). Downstream values of ω are calculated along the subset of four rivers (Coe, Etive, Leven, and Nevis), and as expected, channels cutting quartzite outcrops generate between 2.7 and 3.5 times more power relative to nonquartzite (at $A = 40 \text{ km}^2$), with 95% confidence bands that do not overlap (table 5; fig. 9). Given our findings that channel slope is far more sensitive to substrate erodibility than is channel width, we deduce that channel steepening is predominantly responsible for raising the erosional capacity of streams where they cross resistant rock outcrops.

Discussion

The coupling of lithologically controlled hillslopes with more variable (and partly scale dependent) responses along valley floors accords with the idea that the qualities defining erodibility vary with the erosional agent: ice, water, or mass movement. Does the western Scottish Highlands contain a signature of substrate erodibility? The answer appears to be that the strength of lithological control is spatially dependent, and we frame the following discussion accordingly.

Catchment-Scale Effects of Lithological Controls.

Pervasive lithological control on topography is shown across the entire British Isles (Clayton and Shamon 1998, 1999), and it has long been recognized that ~NE-SW-trending fold and fault structures dictate outlines of relief and topography in Scotland. Given that quartzite outcrops account for just 7% of the total study area, their catchment-scale effects are unexpectedly strong. Our data confirm quantitatively the views of Geikie (1901) and Sissons (1967): major valley troughs in the western Highlands tend to follow lines of substrate weakness, with much of the higher ground formed in quartzite. Smaller (and steeper) catchments are developed in the quartzite-dominated areas that typically fill the space between large fluvial-glacial valley troughs. The lithological control on drainage area and relief does not extend, however, to the hypsometric attributes of the study catchments (cf. Lifton and Chase 1992; Hurtrez et al. 1999). Although lithological effects emerge at smaller spatial scales, catchment H_i values in our study do not correlate with any substrate metrics, and H_i scaling with drainage area applies to a subset of catchments only. Likewise we find no evidence of widespread rock strength equilibrium hillslopes. The analysis of slope angles across the whole landscape shows that quartzite outcrops are steeper relative to the nonquartzites on average, but the two populations overlap considerably.

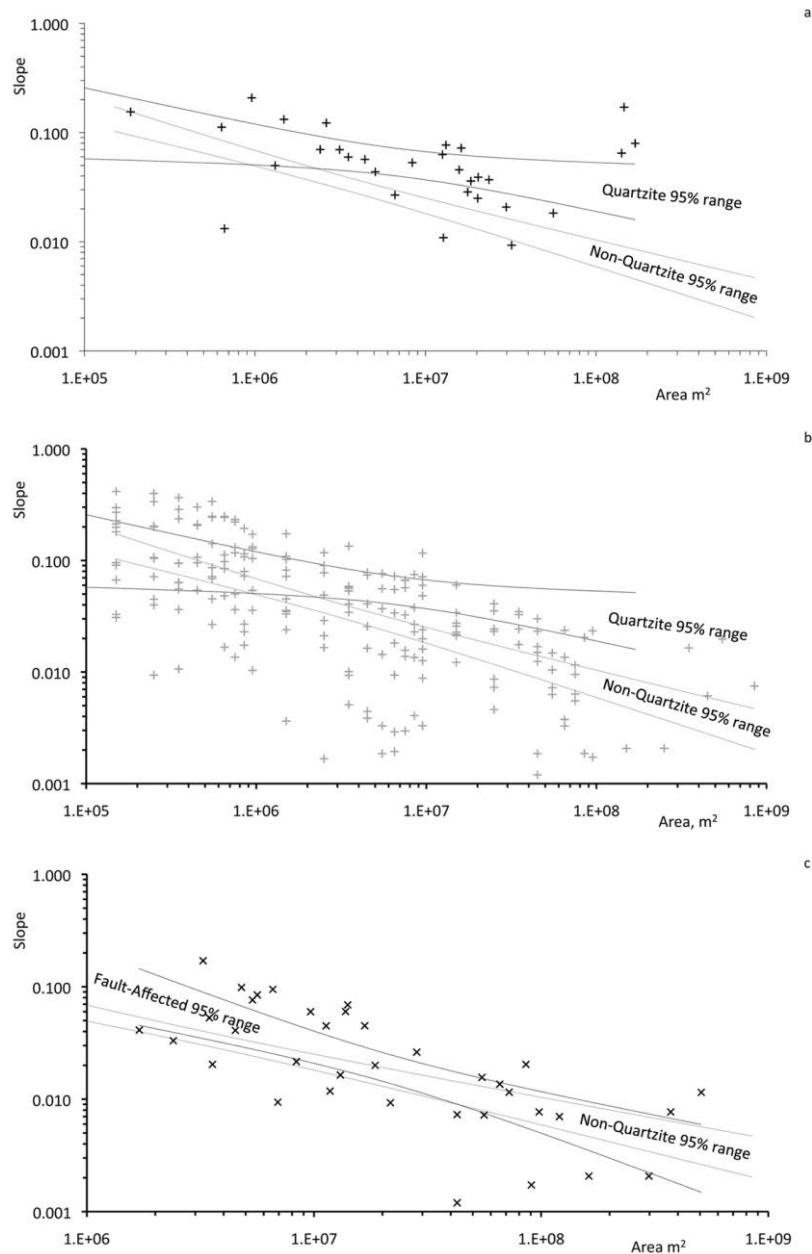


Figure 7. Mean channel slope (log-binned) versus drainage area (log-binned) for channel reaches in 14 rivers crossing. *a*, Quartzite, $S = 1.14A^{-0.194}$; *b*, nonquartzite, $S = 23.9A^{-0.436}$; and *c*, channel reaches within 200 m of faults, $S = 331.7A^{-0.580}$. In each case 95% confidence bands are calculated on the regression (eq. [10]; see table 3). Where quartzite outcrops span multiple area log-bins, average channel slope is plotted separately for each. Multiple quartzite outcrops crossing the same area log-bin are grouped and represented by a single channel slope data point. Excluded are reaches where $A < 0.1 \text{ km}^2$ and where quartzite outcrops are $< 100 \text{ m}$ in channel length.

Channel steepness indices, as derived from equations (3) and (4) are used routinely to infer relative rock uplift rates (e.g., Snyder et al. 2000, 2003a, 2003b; Kobor and Roering 2004; Wobus et al. 2006). Given that acceleration of rock uplift and outcrop of strong rocks are both associated with steeper

landscapes, we tested the inverse, that channel steepness indices can be used to infer differential substrate erodibility where rock uplift is spatially invariant. We find that quartzite outcrop controls steepness (i.e., relief ratio) to some extent at catchment scale, but faults have no effect. This result

Table 4. Regression Analyses of Bedrock Channel Width W versus Drainage Area A (m^2)

| River or substrate | c | b | R^2 | n | Area range (km^2) | $W_r \pm 95\%$ (m) |
|-----------------------------|---------|------|-------|------|------------------------------|-----------------------|
| Coe | 1.71E-4 | .647 | .22 | 862 | 17.5–54.4 | 14.2 \pm .5 |
| Etive | 1.12E-1 | .276 | .23 | 2011 | 6.5–136 | 14.7 \pm .3 |
| Leven ^b | 1.149 | .139 | .20 | 1045 | 4.4–181 | 13.2 \pm .3 |
| Nevis | 2.39E-2 | .363 | .30 | 1907 | 2.2–68.6 | 13.8 \pm .4 |
| All width data ^c | 1.06E-2 | .278 | .26 | 5825 | 2.2–181 | 13.7 \pm .2 |
| Nonquartzite ^d | .107 | .278 | .23 | 5168 | 4.4–162 | 13.9 \pm .2 |
| Quartzite ^e | .129 | .262 | .41 | 657 | 2.2–181 | 12.7 \pm .4 |

Note. The regression analyses are for channel reaches in four rivers (Coe, Etive, Leven, and Nevis) crossing quartzite and non-quartzite, where $W = cA^b$ (eq. [7]).

^a Channel width calculated from regression with 95% confidence interval at a reference drainage area, $A = 40 \text{ km}^2$.

^b No width data available for a 14.5-km reach because of Blackwater Reservoir.

^c All four rivers irrespective of lithology.

^d River reaches crossing nonquartzite rocks.

^e River reaches crossing 10 major quartzite outcrops.

suggests that catchment-scale substrate erodibility can be inferred from equation (4), but local exceptions advise care with its broad-scale application. For instance, S_r fails to account for the large quartzite outcrops associated with major long profile steps on the Leven and Righ (fig. 4). Measures of concavity (C_i and θ) vary widely in the study catchments and are not systematically scaled with drainage area or substrate erodibility. If concavity is influenced by lithological controls, as suggested by VanLaningham et al. (2006) for the Oregon coastal mountains, such effects are restricted to the sub-catchment scale in western Scotland.

Reach-Scale Erosional Capacity of Bedrock Channels. Reach-scale river morphology is mainly a function of the adjustments to erosional capacity that have occurred due to declining sediment supply since deglaciation. Consequently, unlike landforms at the catchment scale, reach-scale landforms preserve fewer inherited features from past regimes.

Channel Width. As with bedrock channel slope, channel width commonly varies locally in response to spatial changes in rock uplift rates and substrate erodibility (e.g., Harbor 1998; Lavé and Avouac 2000, 2001; Snyder et al. 2000, 2003a, 2003b; Montgomery and Gran 2001; Duvall et al. 2004; Finnegan et al. 2005; Whittaker et al. 2007). If width is set by detachment-limited bedrock erosion, then theory predicts that the high erosion thresholds found in strong-rock banks will force comparatively narrow channels. Consistent with this prediction, Montgomery and Gran (2001) describe channel narrowing (but not steepening) along a 5-km reach of the Mokelumne River, California, where it crosses from limestone to unjointed Sierra Nevada granite. However, several other large channel-width data sets from mixed bedrock-alluvial

rivers fail to show systemic channel narrowing across resistant bedrock (namely, Hack 1957; Miller 1958; Brush 1961).

In alluvial settings, channel geometry is a function of discharge, bedload flux, and bank stability (Parker 1979; Ikeda et al. 1988). As pointed out by Montgomery and Gran (2001) and Whipple (2004), the similarity between width-area scaling in bedrock channels and gravel-bed alluvial channels suggests that bedload flux, in particular, plays a key role in determining the width of all channels, irrespective of bank strength inferred from substrate differences. Nonetheless, the detachment-limited behavior implied by the sparse alluvial cover in the Scottish rivers is consistent with channel width being predominantly a function of erosional thresholds at the channel boundary, rather than bedload flux; an interpretation supported by our findings that resistant quartzite yields channels that are 4%–13% narrower than nonquartzite (at $A = 40 \text{ km}^2$). It may be that the role of bedload flux in determining bedrock channel width, postulated by Montgomery and Gran (2001) and Whipple (2004), is important only where substantial alluvial cover on the bed permits increasing transport-limited behavior in the manner of alluvial channels.

Channel Slope. Few of the rivers in western Scotland exhibit the concave-up long profiles expected in the case of steady state erosion of uniform substrate (Whipple and Tucker 1999). Channel slope irregularities in these rivers reflect nonuniform erodibility due to fault-related fracture or erosion resistant rocks (cf. Miller 1991; Wohl and Ikeda 1998; Whipple et al. 2000). The 1.5–6.0-fold channel steepening measured over quartzites (at $A = 40 \text{ km}^2$) diminishes upstream, perhaps with the growing influence of gravity-dependent processes such as debris flows (fig. 7a, 7b). Rivers crossing

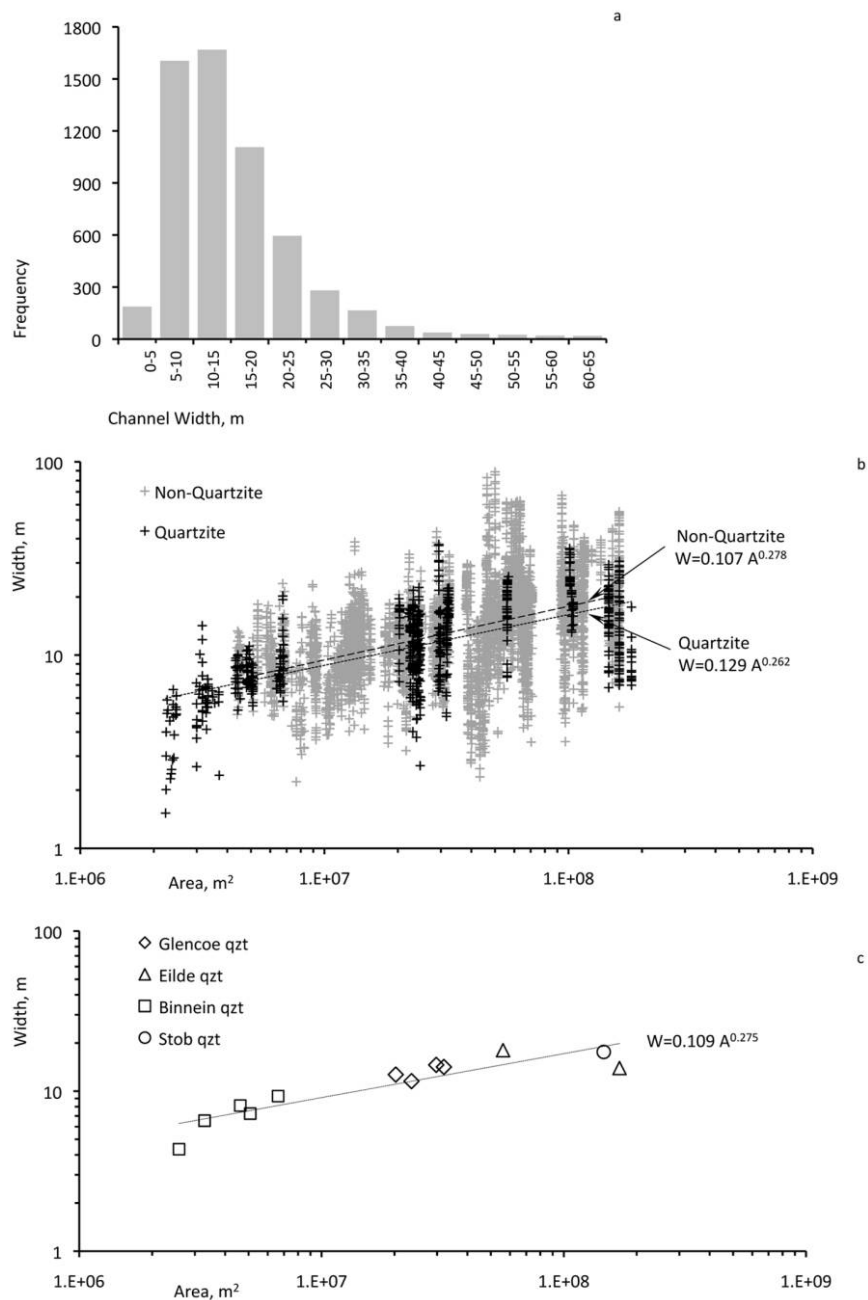


Figure 8. *a*, Frequency histogram of bedrock channel width in four rivers (Coe, Etive, Leven, and Nevis) showing a skewed gamma-type distribution ($n = 5825$); *b*, channel width versus drainage area, with quartzite reaches (*black*) and nonquartzite (*gray*; see table 4 for 95% confidence intervals); *c*, channel width versus drainage area (log-binned) for channel reaches crossing four different “quartzite” lithologies (see table 1).

resistant quartzite outcrops generate between a 2.7- and a 3.5-fold increase in unit stream power, with 4% to 13% of this increase due to channel narrowing and the remainder due to steepening (fig. 9). Such peaks in unit power imply that quartzite has roughly three times the erosional resistance to flu-

vial erosion compared to nonquartzite rocks. Hack (1960, 1975) discussed the potential equilibrium form of topography adjusted according to substrate erodibility. For instance, channel slopes may be adjusted such that long-term erosion rates are equivalent upstream, downstream, and across a litho-

Table 5. Regression Analyses of Unit Stream Power ω (eq. [9]) versus Drainage Area A (m^2)

| Substrate | d | p | R^2 | n | Area range (km^2) | $\omega_r \pm 95\%$ ^a (W/m^2) |
|---------------------------|------|------|-------|------|---------------------------------|---------------------------------------------------------------|
| Quartzite ^b | .727 | .434 | .18 | 657 | 2.2–181 | 1456 \pm 142 |
| Nonquartzite ^c | .023 | .566 | .18 | 5168 | 4.4–162 | 475 \pm 15 |

Note. The regression analyses are for channel reaches in four rivers (Coe, Etive, Leven, and Nevis) crossing quartzite and non-quartzite, where $\omega = dA^p$.

^a Unit stream power calculated from regression with 95% confidence interval at a reference drainage area $A = 40 \text{ km}^2$.

^b River reaches crossing 10 major quartzite outcrops.

^c River reaches crossing nonquartzite rocks.

logical knickpoint (e.g., Jansen 2006). However, the presence of equilibrium is difficult to confirm because where transient knickpoints propagate upstream from weak to strong rocks channel steepening is the result of substrate and transience acting together. The influence of substrate erodibility on transient knickpoints is noted by Crosby and Whipple (2006) on the Waipaoa River, New Zealand, where 76 of 317 post-18-k.yr. knickpoints are located on resistant bedrock. Static, lithologically controlled knickpoints are interpreted by Crosby and Whipple as forming in the wake of transient knickpoints propagating from base level, suggesting that part of the base level signal gets “hung up” at strong-rock outcrops (see also Goldrick and Bishop 1995). This process describes a disequilibrium condition involving differential erosion rates that may lead to important consequences for topography as we discuss below.

Strong-Rock “Barriers” and Postorogenic Relief Decay. By absorbing part or all of the knickpoint base level signal, large strong-rock outcrops have potential to impose a disequilibrium condition whereby long-term erosion rates become suppressed upstream of a strong-rock “barrier” (fig. 10a). It is probably no coincidence that examples of strong-rock barriers buttressing low relief come particularly from non- or postorogenic landscapes, such as Australia’s Eastern Highlands (e.g., Goldrick and Bishop 1995) and southern Africa (e.g., Tooth et al. 2002). A growing number of studies of non- or postorogenic terrain argue that high rock mass strength forces slow erosion rates even in steep, high rainfall terrain; for example, the Western Ghats, India (Gunnell et al. 2003); the Guyana Shield (Stallard 1985, 1988; Edmond et al. 1995); and Sri Lanka (von Blanckenburg et al. 2004). This is not to say that base level disconnection does not occur in orogens—the Tibet plateau is the premier example—but unlike the relatively weak rocks exposed in young orogens (typically uplifted Tertiary marine sediments), long-term terrestrial erosion of non- or postorogenic terrain tends to exhume ancient base-level rocks that are commonly very resistant to

erosion. Coupled with overall tectonic quiescence, the resultant topography is often a sharp reflection of spatial differences in erodibility etched by the structural grain of deformation structures.

The association of bedrock resistance with slow erosion rates also finds support in numerical modeling. The persistence, since the Miocene, of transient river profiles in Australia’s Eastern Highlands is examined by van der Beek and Bishop (2003) and also Stock and Montgomery (1999), with all reporting extremely low K_2 values (eq. [6]), indicating low erosional efficiency and implying that strong rocks suppress bedrock erosion. At a broader scale, Baldwin et al. (2003) argue that the timescale of postorogenic relief decay is set by surface processes driven mainly by rivers (in nonglaciated regions). In a detailed numerical treatment of the relative importance for relief decay of endogenic and exogenic controls, Baldwin et al. find that a model incorporating isostasy, critical shear stress, discharge variability, and either $n > 1$ (eq. [6]) or transition from detachment-limited to transport-limited conditions is best able to explain relief decay timescales exceeding 100 m.yr. Of all model parameters, critical shear stress is the most influential, effecting an ~ 20 -fold increase in relief decay time. The role of substrate erodibility is expressed directly in the critical shear stress for bedrock erosion under detachment-limited conditions and indirectly for transport-limited conditions via sediment entrainment thresholds. Thus, the high rock-mass strength typical of non- or postorogenic mountain belts appears to be fundamental to landscape evolution.

The idea of strong-rock barriers impeding knickpoint retreat takes the modeling implications further because under detachment-limited conditions, new base level information must first propagate through the river network via knickpoints before the signal is transmitted to hillslopes. We postulate that propagation of multiple transient knickpoints over time causes lithological knickpoints to “amplify” in steepness or height and that this effect should be measurable in reaches close to base level

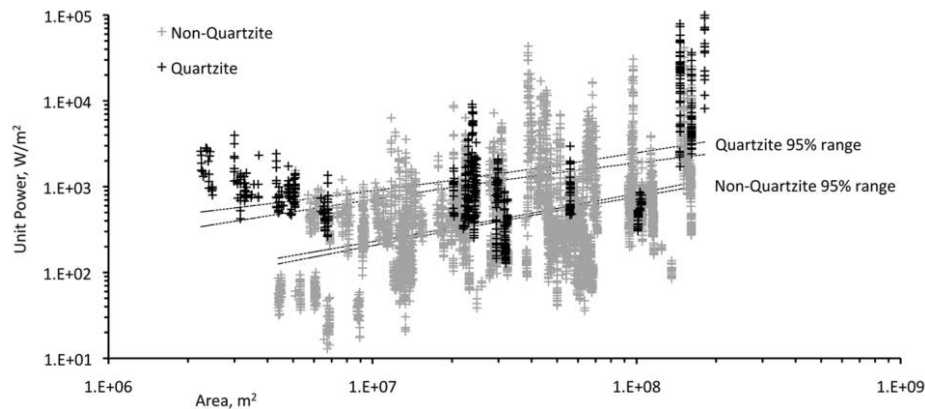


Figure 9. Unit stream power (eq. [9]) versus drainage area for 10 major quartzite outcrops (*black*) and nonquartzites (*gray*), from four rivers (Coe, Etive, Leven, and Nevis), with 95% confidence bands calculated on the regressions (see table 5).

(fig. 10a). Ongoing knickpoint amplification progressively increases relief amplitude as strong-rock barriers isolate the landscape above from the effects of base level fluctuations (Twidale 1976, 1991). In order to detect the presence of amplified lithological knickpoints in areas close to base level, we plot trends in total stream power (i.e., the slope-discharge product) along the subset of four rivers in western Scotland (fig. 10b). For nonquartzite reaches the 95% confidence band traces a decline in total power downstream, whereas quartzite reaches show pronounced rise in total power as base level is approached. Given that transient knickpoints caused by Holocene glacio-isostatic rebound are excluded from our analysis, we interpret the rise in total power as the cumulative result of successive interglacial periods consistent with knickpoint amplification at strong-rock barriers. The lithological knickpoints shown in figure 4 may be good examples of this amplification, as both are <2 km from their respective river outlets.

Glacial and Postglacial Inheritance. Differential erodibility is commonly invoked to explain glacial valley cross sections that range from narrow deep troughs in resistant rocks to broader open troughs cut in weaker rocks (e.g., Augustinus 1992, 1995). In long profile, glacial valleys typically contain multiple steepenings separated by low-gradient reaches, and the steepness index outlier (11) in figure 6i is probably one such effect. Given that all glacial steps (i.e., glacial knickpoints) become fluvial knickpoints following ice retreat, polygenetic inheritance is likely to be a factor in the irregular long profiles in the study area, including those depicted in figure 10. The extent to which these long

profiles are “glacial” or “fluvial” is difficult to unravel, but it seems reasonable to assume that the strength of glacial erosion declines downstream as fluvial attributes strengthen toward base level (fig. 3). The erosional capacity of valley glaciers is thought to be proportional to basal shear stress or sliding velocity (Hallet 1981; Anderson et al. 2006). We postulate that the generally weak catchment-scale lithological control in western Scotland (fig. 6) may be the product of successive glaciations involving valley glaciers that tended to erode all rock types uniformly, irrespective of rock mass strength, thanks to a large excess of shear stress at the glacier base. During interglacial stages, by contrast, we contend that detachment-limited rivers effectively amplify erodibility differences. Such an interpretation is consistent with the strengthening of the lithological signal downstream shown in figure 10.

Based on observations of non- or postorogenic landscapes elsewhere, which show widespread detachment-limited conditions, we assume that such conditions are representative of sediment supply rates under nonglacial regimes. Sediment production increases during glaciations (Church and Ryder 1972; Ballantyne 2002), representing a major departure from the relatively low “background” sediment supply rates in tectonically quiescent landscapes. Immediately following ice retreat in Scotland, greater sediment supply probably forced a period of transport-limited conditions as rivers reworked the valley floor deposits left by glaciers. Judging by the remnants of fluvio-glacial terraces, valley floor sediments rarely exceeded 4 m thick, and cosmogenic ^{10}Be concentrations in exposed bedrock strath terraces indicate widespread detachment-limited con-

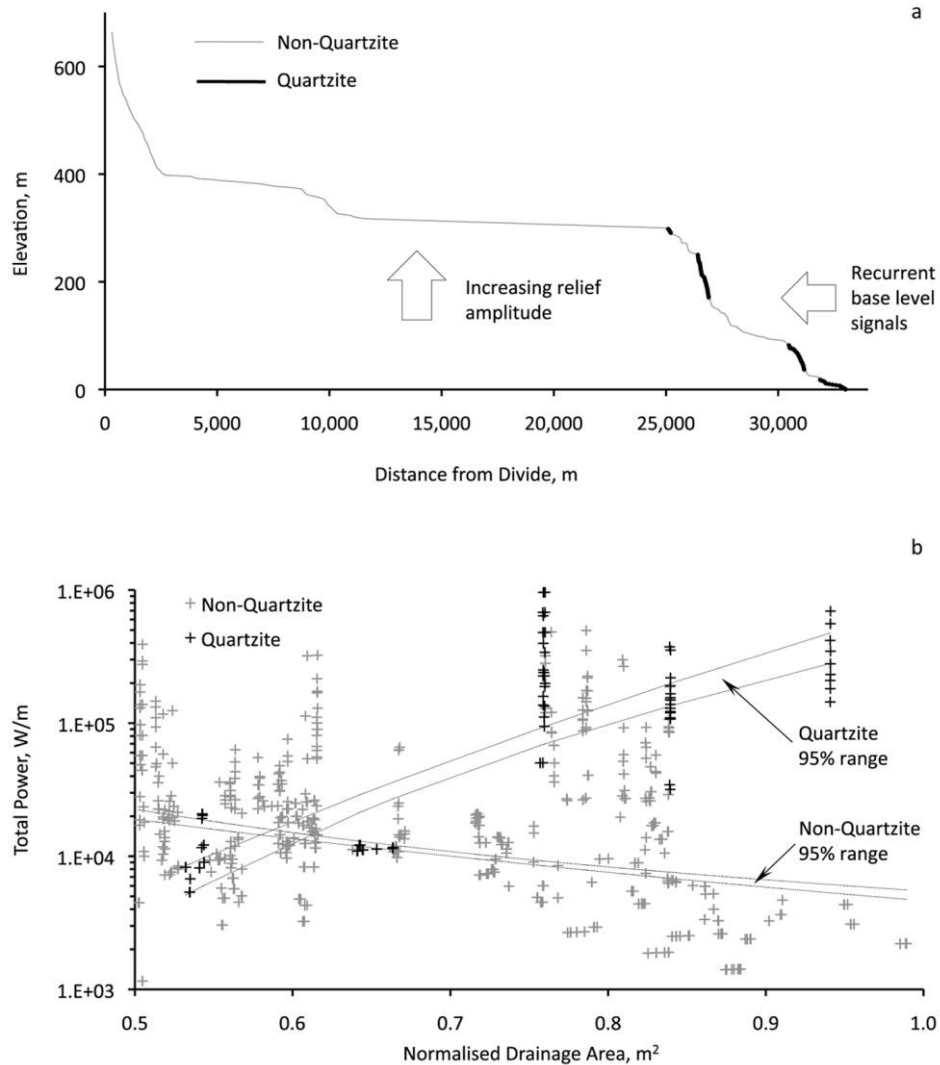


Figure 10. *a*, River Leven long profile, with lithological knickpoints developed at quartzite outcrops. Such resistant outcrops may foster differential rates of erosion in the landscape by impeding the transmission of base level information to headwater areas and therefore increasing relief amplitude. *b*, Total stream power (Ω) versus normalized drainage area spanning the downstream half of four river networks (normalized drainage area of 1.0 marks the river outlets of the Coe, Etive, Leven, and Nevis), with quartzite outcrops (*black*), nonquartzites (*gray*), and 95% confidence bands calculated on the regressions. Note that $\Omega = \gamma QS$, where γ is the specific weight of water (9807 N/m^3), and Q is calculated from equation (1).

ditions from the early Holocene (J. D. Jansen, unpublished manuscript). In western Scotland, therefore, any transport-limited phase arising from paraglacial sediment supply was probably brief, and the return of large areas of exposed bedrock reasserted the lithological control of topographic form.

Conclusions

Substrate erodibility exerts pronounced control on landscape morphology in western Scotland, but the

strength of this control varies with spatial scale and the landform in question. Building on previous work showing that differential erodibility governs much of the regional-scale topographic relief of the British Isles (Clayton and Shamon 1998, 1999), our analyses conducted at the catchment and reach scales introduce some key refinements. Major valley troughs, including fjords, trace fault-related zones of weakness and nonquartzite rocks, leaving much of the higher ground formed in quartzite.

Where rock uplift is spatially invariant, catchment-scale erodibility can be successfully inferred from steepness indices (i.e., channel steepness index, relief ratio, and mean slope angle), though local exceptions could confound a general application of this approach.

Responses to substrate erodibility at the reach scale are sharply divided between channel width and slope, the latter being more sensitive by far. A unit stream power-based model indicates that rivers increase their erosional capacity at quartzite outcrops by a factor of 2.7–3.5 (at 40 km²), yet only 4% to 13% of this is due channel narrowing. Furthermore, increased steepness at quartzite outcrops does not lead to increased topographic relief overall, because strong-rock barriers exert local base level control on reaches upstream. Such base level effects pose a challenge for modeling river profiles, but our analyses show that the use of generic width-area scaling in bedrock river incision models offers a valid approximation of unit stream power, provided that rock uplift can be assumed to be spatially in-

variant. We find that channel width scales with drainage area in a similar fashion for all single-thread rivers subject to predominantly transport-limited conditions. But where meager sediment supply provides sparse alluvial cover, such as in western Scotland, channel width is a function of erosional thresholds associated with bedrock detachment and coarse debris lining the bed.

ACKNOWLEDGMENTS

This work was conducted while J. Jansen held a postdoctoral fellowship linked to a Natural Environment Research Council (NERC) grant (NE/C510416/1) awarded to P. Bishop, T. Hoey, and J. Jansen, and a NERC postdoctoral fellowship (NE/EO14143/1) awarded to J. Jansen. A. T. Codilean held a postdoctoral fellowship linked to an Arts and Humanities Research Council grant awarded to P. Bishop and T. Fallick (AHRC 119196). The NextMAP digital elevation data was provided by the NERC.

REFERENCES CITED

- Anderson, R. S.; Molnar, P.; and Kessler, M. A. 2006. Features of glacial valley profiles simply explained. *J. Geophys. Res.* 111:F01004, doi:10.1029/2005JF000344.
- Annandale, G. W. 1995. Erodibility. *J. Hydraul. Res.* 33: 471–494.
- Augustinus, P. C. 1992. The influence of rock mass strength on glacial valley cross-profile morphometry: a case study from the Southern Alps of New Zealand. *Earth Surf. Proc. Landforms* 17:39–51.
- . 1995. Glacial valley cross-profile development: the influence of in situ rock stress and rock mass strength, with examples from the Southern Alps, New Zealand. *Geomorphology* 14:87–97.
- Bailey, E. B., and Maufe, H. B. 1916. The geology of Ben Nevis and Glen Coe and the surrounding country (2nd ed., revised by E. B. Bailey). *Memoirs of the Geological Survey of Great Britain*. Edinburgh, Her Majesty's Stationery Office, 307 p.
- Baldwin, J.; Whipple, K. X.; and Tucker, G. E. 2003. Implications of the shear stress river incision model for the timescale of postorogenic decay of topography. *J. Geophys. Res.* 108:2158, doi:10.1029/2001JB000550.
- Ballantyne, C. K. 2002. Paraglacial geomorphology. *Quat. Sci. Rev.* 21:1935–2017.
- Bishop, P.; Hoey, T. B.; Jansen, J. D.; and Artza, I. L. 2005. Knickpoint recession rate and catchment area: the case of uplifted rivers in eastern Scotland. *Earth Surf. Proc. Landforms* 30:767–778, doi:10.1002/esp.1191.
- Boulton, G. S.; Peacock, J. D.; and Sutherland, D. G. 2002. Quaternary. *In* Trewin, N. H., ed. *The geology of Scotland*. London, Geological Society, p. 409–430.
- Brocklehurst, S. H., and Whipple, K. X. 2007. Response of glacial landscapes to spatial variations in rock uplift rate. *J. Geophys. Res.* 112:F02035, doi:10.1029/2006JF000667.
- Brookfield, M. E. 1998. The evolution of the great river systems of southern Asia during the Cenozoic India-Asia collision: rivers draining southwards. *Geomorphology* 22:285–312.
- Brush, L. M. 1961. Drainage basins, channels, and flow characteristics of selected streams in central Pennsylvania. *Physiographic and Hydrographic Studies of Rivers*. U.S. Geol. Surv. Prof. Pap. 282F:145–181.
- Burbank, D. W.; Leland, J.; Fielding, E.; Anderson, R. S.; Brozovic, N.; Reid, M. R.; and Duncan, C. 1996. Bedrock incision, rock uplift and threshold hillslopes in the northwestern Himalayas. *Nature* 379:505–510.
- Chen, Y.-C.; Sung, Q.; and Cheng, K.-Y. 2003. Along-strike variations of morphometric features in the Western Foothills of Taiwan: tectonic implications based on stream-gradient and hypsometric analysis. *Geomorphology* 56:109–137, doi:10.1016/S0169-555X(03)00059-X.
- Church, M., and Ryder, J. M. 1972. Paraglacial sedimentation: a consideration of fluvial processes conditioned by glaciation. *Geol. Soc. Am. Bull.* 83:3059–3072.
- Clayton, K. M. 1974. Zones of glaciation. *In* Brown, E. H., and Waters, R. S., eds. *Progress in geomorphology*. Inst. Br. Geogr. Spec. Publ. 7:163–176.
- Clayton, K. M., and Shamon, N. 1998. A new approach to the relief of Great Britain II. A classification of rocks

- based on relative resistance to denudation. *Geomorphology* 25:155–171.
- . 1999. A new approach to the relief of Great Britain III. Derivation of the contribution of neotectonic movements and exceptional regional denudation to the present relief. *Geomorphology* 27:173–189.
- Crickmay, C. H. 1975. The hypothesis of unequal activity. In Melhorn, W. M., and Flemal, R. C., eds. *Theories of landform development*. Publications in Geomorphology. Binghamton, State University of New York, p. 103–109.
- Crosby, B. T., and Whipple, K. X. 2006. Knickpoint initiation and distribution within fluvial networks: 236 waterfalls in the Waipaoa River, North Island, New Zealand. *Geomorphology* 82:16–38, doi:10.1016/j.geomorph.2005.1008.1023.
- Davis, W. M. 1899. The geographical cycle. *Geograph. J.* 14:481–504.
- Dietrich, W. E.; Bellugi, D.; Heimsath, A. M.; Roering, J. J.; Sklar, L. S.; and Stock, J. D. 2003. Geomorphic transport laws for predicting the form evolution of landscapes. In Wilcock, P. R., and Iverson, R., eds. *Prediction in geomorphology*. Am. Geophys. Union Geophys. Monogr. 135:103–132.
- Duvall, A.; Kirby, E.; and Burbank, D. 2004. Tectonic and lithologic controls on bedrock channel profiles and processes in coastal California. *J. Geophys. Res.* 109: F03002, doi:10.29/2003JF000086.
- Edmond, J. M.; Palmer, M. R.; Measures, C. I.; Grant, B.; and Stallard, R. F. 1995. The fluvial geochemistry and denudation rate of the Guyana Shield in Venezuela, Colombia, and Brazil. *Geochim. Cosmochim. Acta* 59: 3301–3325.
- Fernandes, N. F., and Dietrich, W. E. 1997. Hillslope evolution by diffusive processes: the timescale for equilibrium adjustments. *Water Resour. Res.* 33:1307–1318.
- Finnegan, N. J.; Roe, G.; Montgomery, D. R.; and Hallet, B. 2005. Controls on the channel width of rivers: implications for modelling fluvial incision of bedrock. *Geology* 33:229–232, doi:10.1130/G21171.1.
- Firth, C. R., and Stewart, I. S. 2000. Postglacial tectonics of the Scottish glacio-isostatic uplift centre. *Quat. Sci. Rev.* 19:1469–1493.
- Flint, J. J. 1974. Stream gradient as a function of order, magnitude, and discharge. *Water Resour. Res.* 10:969–973.
- Gardner, T. W. 1983. Experimental study of knickpoint and longitudinal profile evolution in cohesive, homogeneous material. *Geol. Soc. Am. Bull.* 94:664–672.
- Geikie, A. 1901. *The scenery of Scotland* (3rd ed.). London, Macmillan, 540 pp.
- Gilbert, G. K. 1877. *Report on the geology of the Henry Mountains*. Washington, DC, Government Printing Office.
- Goldrick, G., and Bishop, P. 1995. Differentiating the roles of lithology and uplift in the steepening of bedrock river long profiles: an example from southeastern Australia. *J. Geol.* 103:227–221.
- Golledge, N. R.; Fabel, D.; Everest, J. D.; Freeman, S.; and Binnie, S. 2007. First cosmogenic ^{10}Be age constraint on the timing of Younger Dryas glaciation and ice cap thickness, western Scottish Highlands. *J. Quat. Sci.* 22: 785–791, doi:10.1002/jqs.1113.
- Gregory, J. W. 1927. The fiords of the Hebrides. *Geogr. J.* 69:193–212.
- Gunnell, Y.; Gallagher, K.; Carter, A.; Widdowson, M.; and Hurford, A. J. 2003. Denudation history of the continental margin of western peninsular India since the early Mesozoic—reconciling apatite fission-track data with geomorphology. *Earth Planet. Sci. Lett.* 215: 187–201.
- Hack, J. T. 1957. Studies of longitudinal stream profiles in Virginia and Maryland. *Shorter Contributions to General Geology*. U.S. Geol. Surv. Prof. Pap. 294-B:45–97.
- . 1960. Interpretations of erosional topography in humid temperate regions. *Am. J. Sci.* 258:80–97.
- . 1975. Dynamic equilibrium and landscape evolution. In Melhorn, W. M., and Flemal, R. C., eds. *Theories of landform development*. Publications in Geomorphology. Binghamton, State University of New York, p. 87–102.
- Hallet, B. 1981. Glacial abrasion and sliding: their dependence on the debris concentration in basal ice. *Ann. Glaciol.* 2:23–28.
- Harbor, D. J. 1998. Dynamic equilibrium between an active uplift and the Sevier River, Utah. *J. Geol.* 106: 181–194.
- Harris, A. L. 1991. The growth and structure of Scotland. In Craig, G. Y. ed. *The geology of Scotland* (3rd ed.). London, Geological Society, p. 1–24.
- Harris, A. L.; Haselock, P. J.; Kennedy, M. J.; Mendum, J. R.; Long, C. B.; Winchester, J. A.; and Tanner, P. W. G. 1994. The Dalradian Supergroup in Scotland, Shetland and Ireland. In Gibbons, W., and Harris, A. L., eds. *Revised correlation of Precambrian rocks in the British Isles*. *Geol. Soc. Lond. Spec. Rep.* 22:33–53.
- Holland, W. N., and Pickup, G. 1976. Flume study of knickpoint development in stratified sediment. *Geol. Soc. Am. Bull.* 87:76–82.
- Horn, B. K. P. 1981. Hill shading and the reflectance map. *Proc. IEEE* 69:14–47.
- Howard, A. D. 1980. Thresholds in river regimes. In Coates, D. R., and Vitek, J. D., eds. *Thresholds in geomorphology*. Boston, Allen & Unwin, p. 227–258.
- Howard, A. D.; Dietrich, W. E.; and Seidl, M. A. 1994. Modeling fluvial erosion on regional to continental scales. *J. Geophys. Res.* 99:13,971–13,986.
- Howard, A. D., and Kerby, G. 1983. Channel changes in badlands. *Geol. Soc. Am. Bull.* 94:739–752.
- Hurtrez, J.-E.; Sol, C.; and Lucazeau, F. 1999. Effect of drainage area on hypsometry from an analysis of small-scale drainage basins in the Siwalik Hills (central Nepal). *Earth Surf. Proc. Landforms* 24:799–808.
- Ikeda, S.; Parker, G.; and Kimura, Y. 1988. Stable width and depth of straight gravel rivers with heterogeneous bed materials. *Water Resour. Res.* 24:713–722.
- Jansen, J. D. 2006. Flood magnitude-frequency and lithologic control on bedrock river incision in post-oro-

- genic terrain. *Geomorphology* 82:39–57, doi:10.1016/j.geomorph.2005.08.018.
- Jenson, S. K., and Domingue, J. O. 1988. Extracting topographic structure from digital elevation data for geographic information system analysis. *Photogrammetr. Eng. Remote Sens.* 54:593–600.
- Kirby, E.; Whipple, K. X.; Tang, W.; and Chen, Z. 2003. Distribution of active rock uplift along the eastern margin of the Tibetan Plateau: inferences from bedrock channel longitudinal profiles. *J. Geophys. Res.* 108(B4):2217, doi:10.1029/2001JB000861.
- Kobor, J. S., and Roering, J. J. 2004. Systematic variation of bedrock channel gradients in the central Oregon Coast Range: implications for rock uplift and shallow landsliding. *Geomorphology* 62:239–256, doi:10.1016/j.geomorph.2004.02.013.
- Korup, O. 2008. Rock type leaves topographic signature in landslide-dominated mountain ranges. *Geophys. Res. Lett.* 35:L11402, doi:10.1029/2008GL034157.
- Kühni, A., and Pfiffner, O. A. 2001. The relief of the Swiss Alps and adjacent areas and its relation to lithology and structure: topographic analysis from a 250-m DEM. *Geomorphology* 41:285–307.
- Lague, D.; Davy, P.; and Crave, A. 2000. Estimating uplift rate and erodibility from the area-slope relationship: examples from Brittany (France) and numerical modelling. *Phys. Chem. Earth A* 25:543–548.
- Lavé, J., and Avouac, J. P. 2000. Active folding of fluvial terraces across the Siwaliks Hills, Himalayas of central Nepal. *J. Geophys. Res.* 105:5735–5770.
- . 2001. Fluvial incision and tectonic uplift across the Himalayas of central Nepal. *J. Geophys. Res.* 106:26,561–26,591.
- Leopold, L. B., and Maddock, T. 1953. The hydraulic geometry of stream channels and some physiographic implications. *U.S. Geol. Surv. Prof. Pap.* 282A, 57 p.
- Lifton, N. A., and Chase, C. G. 1992. Tectonic, climatic and lithologic influences on landscape fractal dimension and hypsometry: implications for landscape evolution in the San Gabriel Mountains, California. *Geomorphology* 5:77–114.
- Miller, J. P. 1958. High mountain streams: effects of geology on channel characteristics and bed material. *New Mexico Institute of Mining and Technology Memoir* 4. Socorro, NM, State Bureau of Mines and Mineral Resources, 53 pp.
- Miller, J. R. 1991. The influence of bedrock geology on knickpoint development and channel-bed degradation along downcutting streams in south-central Indiana. *J. Geol.* 99:591–605.
- Moglen, G. E., and Bras, R. L. 1995. The effect of spatial heterogeneities on geomorphic expression in a model of basin evolution. *Water Resour. Res.* 31:2613–2623.
- Molnar, P.; Anderson, R. S.; and Anderson, S. P. 2007. Tectonics, fracturing of rock, and erosion. *J. Geophys. Res.* 112:F03014., doi:10.1029/2005JF000433.
- Montgomery, D. R. 2004. Observations on the role of lithology in strath terrace formation and bedrock channel width. *Am J. Sci.* 304:454–476.
- Montgomery, D. R., and Brandon, M. T. 2002. nonlinear controls on erosion rates in tectonically active mountain ranges. *Earth Planet. Sci. Lett.* 201:481–489.
- Montgomery, D. R., and Gran, K. B. 2001. Downstream hydraulic geometry of bedrock channels. *Water Resour. Res.* 37:1841–1846.
- Parker, G. 1979. Hydraulic geometry of active gravel rivers. *J. Hyd. Div. ASCE* 105:1185–1201.
- Pazzaglia, F. J., and Gardner, T. W. 1994. Late Cenozoic flexural deformation of the middle U.S. Atlantic passive margin. *J. Geophys. Res.* 99:12,143–12,157.
- Persano, C.; Barfod, D. N.; Stuart, F. M.; and Bishop, P. 2007. Constraints on early Cenozoic underplating-driven uplift and denudation of western Scotland from low temperature thermochronometry. *Earth Planet. Sci. Lett.* 263:404–419, doi:10.1016/j.epsl.2007.09.016.
- Schmidt, K. M., and Montgomery, D. R. 1995. Limits to relief. *Science* 270:617–620.
- Seidl, M. A., and Dietrich, W. E. 1992. The problem of channel erosion into bedrock. *In* Schmidt, K.-H., and de Ploey, J., eds. *Functional geomorphology: landform analysis and Models*. *Catena* 23(suppl.):101–124.
- Selby, M. J. 1980. A rock mass strength index classification for geomorphic purposes: with tests from Antarctica and New Zealand. *Z. Geomorph. N.F.* 24:31–51.
- . 1993. *Hillslope materials and processes* (2nd ed.). Oxford, Oxford University Press, 451 p.
- Shackleton, N. J.; Backman, J.; Zimmerman, H.; Kent, D. V.; Hall, M. A.; Roberts, D. G.; Schnitker, D.; et al. 1984. Oxygen isotope calibration of the onset of ice-rafting and history of glaciation in the North Atlantic region. *Nature* 307:620–623.
- Shennan, I.; Lambeck, K.; Horton, B.; Innes, J.; Lloyd, J.; McArthur, J.; Purcell, T.; and Rutherford, M. 2000. Late Devensian and Holocene records of relative sea-level changes in northwest Scotland and their implications for glacio-isostatic modelling. *Quat. Sci. Rev.* 19:1103–1135.
- Sissons, J. B. 1967. *The evolution of Scotland's scenery*. Edinburgh, Oliver & Boyd, 259 p.
- Sklar, L., and Dietrich, W. E. 1998. River longitudinal profiles and bedrock incision models: stream power and the influence of sediment supply. *In* Tinkler, K. J., and Wohl, E. E., eds. *Rivers over rock: fluvial processes in bedrock channels*. *Am. Geophys. Union Geophys. Monogr.* 107:237–260.
- . 2001. Sediment supply, grain size and rock strength controls on rates of river incision into bedrock. *Geology* 29:1087–1090.
- Snyder, N. P.; Whipple, K. X.; Tucker, G. E.; and Merritts, D. J. 2000. Landscape response to tectonic forcing: DEM analysis of stream profiles in the Mendocino triple junction region, northern California. *Geol. Soc. Am. Bull.* 112:1250–1263.
- . 2003a. Channel response to tectonic forcing and hydrology in the Mendocino triple junction region, northern California. *Geomorphology* 53:97–127, doi:10.1016/S0169-555X(02)00349-5.
- . 2003b. Importance of a stochastic distribution of floods and erosion thresholds in the bedrock river in-

- cision problem. *J. Geophys. Res.* 108:2117, doi:10.1029/2001JB001655.
- Stallard, R. F. 1985. River chemistry, geology, geomorphology, and soils in the Amazon and Orinoco basins. *In* Drever, J. I., ed. *The chemistry of weathering*. Springer, New York, p. 293–316.
- . 1988. Weathering and erosion in the humid tropics. *In* Lerman, A., and Meybeck, M., eds. *Physical and chemical weathering in geochemical cycles*. New York, Springer, p. 225–246.
- Stephenson, R. 1984. Flexural models of continental lithosphere based on long-term erosional decay of topography. *Geophys. J. R. Astron. Soc.* 77:385–413.
- Stock, J. D., and Montgomery, D. R. 1999. Geologic constraints on bedrock river incision using the stream power law. *J. Geophys. Res.* 104:4983–4993.
- Stuart, F. M.; Ellam, R. M.; Harrop, P. J.; Fitton, J. G.; and Bell, B. R. 2000. Constraints on mantle plumes from the helium isotopic composition of basalts from the British Tertiary Igneous Province. *Earth Planet. Sci. Lett.* 177:273–285.
- Sugden, D. E., and John, B. S. 1976. *Glaciers and landscape: a geomorphological approach*. New York, Arnold.
- Summerfield, M. A. 1991. *Global geomorphology*. Harlow, Longman, 537 pp.
- Tarboton, D. G. 1997. A new method for the determination of flow directions and upslope areas in grid digital elevation models. *Water Resour. Res.* 33:309–319.
- Thomas, C. W.; Gillespie, M. R.; and Jordan, C. J. 2004. Geological structure and landscape of the Cairngorms Mountains. *Scottish Natural Heritage Commissioned Rep. 64*. Perth, Scottish Natural Heritage, 128 p.
- Tomkin, J. H.; Brandon, M. T.; Pazzaglia, F. J.; Barbour, J. R.; and Willett, S. D. 2003. Quantitative testing of bedrock incision models for the Clearwater River, NW Washington State. *J. Geophys. Res.* 108(B6):2308, doi:10.1029/2001JB000862.
- Tooth, S.; McCarthy, T. S.; Brandt, D.; Hancox, P. J.; and Morris, R. 2002. Geological controls on the formation of alluvial meanders and floodplain wetlands: the example of the Klip River, eastern Free State, South Africa. *Earth Surf. Proc. Landforms* 27:797–815, doi:10.1002/esp.353.
- Tucker, G. E., and Whipple, K. X. 2002. Topographic outcomes predicted by stream erosion models: sensitivity analysis and intermodel comparison. *J. Geophys. Res.* 107:2179, doi:10.1029/2001JB000162.
- Twidale, C. R. 1976. On the survival of palaeoforms. *Am. J. Sci.* 276:77–94.
- . 1991. A model of landscape evolution involving increased and increasing relief amplitude. *Z. Geomorphol.* 35(suppl.):85–109.
- van der Beek, P., and Bishop, P. 2003. Cenozoic river profile development in the Upper Lachlan catchment (SE Australia) as a test of quantitative fluvial incision models. *J. Geophys. Res.* 108(B6):2309, doi:10.1029/2002JB002125.
- VanLaningham, S.; Meigs, A.; and Goldfinger, C. 2006. The effects of rock uplift and rock resistance on river morphology in a subduction zone forearc, Oregon, USA. *Earth Surf. Proc. Landforms* 31:1257–1279, doi:10.1002/esp.1326.
- von Blanckenburg, F.; Hewawasam, T.; and Kubik, P. W. 2004. Cosmogenic nuclide evidence for low weathering and denudation in the wet, tropical highlands of Sri Lanka. *J. Geophys. Res.* 109:F03008, doi:10.1029/2003JF000049.
- Weissel, J. K., and Seidl, M. A. 1997. Influence of rock strength properties on escarpment retreat across passive continental margins. *Geology* 25:631–634.
- Whipple, K. X. 2004. Bedrock rivers and the geomorphology of active orogens. *Annu. Rev. Earth Planet. Sci.* 32:151–185.
- Whipple, K. X.; Hancock, G. S.; and Anderson, R. S. 2000. River incision into bedrock: Mechanics and relative efficacy of plucking, abrasion, and cavitation. *Geol. Soc. Am. Bull.* 112:490–503.
- Whipple, K. X., and Tucker, G. E. 1999. Dynamics of the stream power river incision model: implications for height limits of mountain ranges, landscape response timescales and research needs. *J. Geophys. Res.* 104:17,661–17,674.
- Whittaker, A. C.; Cowie, P. A.; Tucker, G. E.; and Roberts, G. P. 2007. Bedrock channel adjustment to tectonic forcing: implications for predicting river incision rates. *Geology* 35:103–106, doi:10.1130/G23106A.1.
- Wobus, C.; Whipple, K. X.; Kirby, E.; Snyder, N.; Johnson, J.; Spyropolou, K.; Crosby, B.; and Sheehan, D. 2006. Tectonics from topography: procedures, promise, and pitfalls. *In* Willett, S. D.; Hovius, N.; Brandon, M. T.; and Fisher, D. M., eds. *Tectonics, climate and landscape evolution*. *Geol. Soc. Am. Spec. Pap.* 398:55–74, doi:10.1130/2006.2398(04).
- Wohl, E. E.; Greenbaum, N.; Schick, A. P.; and Baker, V. R. 1994. Controls on bedrock channel incision along Nahal Paran, Israel. *Earth Surf. Proc. Landforms* 19:1–13.
- Wohl, E. E., and Ikeda, H. 1998. Patterns of bedrock channel erosion on the Boso Peninsula, Japan. *J. Geol.* 106:331–345.